ANL-77-81

ANL-77-81

# A SURVEY OF NUMERICAL METHODS FOR HYDRAULIC TRANSIENTS

by

G. K. Leaf and T. C. Chawla


ARGONNE NATIONAL LABORATORY, ARGONNE, ILLINOIS

Prepared for the U. S. DEPARTMENT OF ENERGY
under Contract W-31-109-Eng-38

Printed in the United States of America
Available from
National Technical Information Service
U. S. Department of Commerce
5285 Port Royal Road
Springfield, Virginia 22161
Price: Printed Copy $6.00; Microfiche $3.00

Distribution Category:
Mathematics and Computers
(UC-32)

ANL-77-81

ARGONNE NATIONAL LABORATORY
9700 South Cass Avenue
Argonne, Illinois 60439

# A SURVEY OF NUMERICAL METHODS FOR HYDRAULIC TRANSIENTS

by

G. K. Leaf
Applied Mathematics Division

and

T. C. Chawla
Reactor Analysis and Safety Division

October 1977

TABLE OF CONTENTS

## LIST OF FIGURES



## LIST OF TABLES

# A SURVEY OF NUMERICAL METHODS FOR HYDRAULIC TRANSIENTS

by

G. K. Leaf and T. C. Chawla

ABSTRACT

The finite difference methods of Lax, Lax-Wendroff (two-step), donor cell type and finite-element method using Galerkin procedure with B-splines as approximating functions are compared with the method of characteristics for the solution of water-hammer transients as typified by valve closure problems. From the point of view of accuracy, the two-step Lax-Wendroff method and the method of characteristics are comparable and produce the best results. The Lax methods fair worst. The donor cell type and the Galerkin procedure with quadratic B-spline basis as approximating functions display roughly the same accuracy. From the comparison presented, it appears that Galerkin technique offers no substantial advantage over the other finite-difference methods except that of ease in handling boundary conditions as compared to finite-difference methods.

## 1. INTRODUCTION

The numerical treatment utilizing various numerical schemes of the dynamic phenomena encountered in the confined flow of fluids through pipes and other conduits connecting two or more regions of space is the object of study in the present paper. The particular dynamic phenomena of interest in the present study are those pertaining to pressure transients in hydraulic pipelines that demonstrate both inertial and elastic effects; these pressure transients are commonly known as waterhammers. Waterhammers can, for example, be caused by sudden closure of a valve in a pipeline which is running full at steady state prior to closure; waterhammers can also be caused by suddenly opening the valve in a pipeline which contains a fluid under pressure. The unsteady flow problem in natural gas systems as initiated by the time variant nature of loads at distribution points and from adjustments made by the system operator in reacting to the demands of the system, afford another example of waterhammer-like problems. In a liquid-metal cooled fast breeder reactor

(LMFBR), Sodium-water reaction like column separation during waterhammer transient results in generation of high pressures and consequently waterhammer like transients.

The basic equations governing the unsteady motion of a fluid in a pipe are the conservation equations of mass, momentum, the equation of state for the liquid, and the elastic properties of the pipe. The resulting system of equations lead to a one-dimensional hyperbolic system of partial differential equations. The most popular method employed is the method of characteristics. However, in the several years of development of numerical procedures for solution on the digital computers, it is a well known fact that generally no single method is able to offer a decisive advantage for all types of conditions occurring in a given class of problems. For example, the two-step Lax-Wendroff method when used in the solution of equations governing pressure pulsations occurring in a positive displacement engine and compressor systems due to the inherently intermittent nature of the gas flow was found to be more accurate and required less computer time than the method of characteristics which is traditionally employed for solution of this problem [1]. The purpose of the present paper is to review and catalogue various methods that can potentially be used for the solution of the waterhammer transients or more general unsteady one-dimensional flow problems. In addition, we have also introduced the use of the finite element method using a Galerkin procedure for this class of problems which, to the best of our knowledge, has not been attempted previously. The motivation for investigating the use of this method is twofold. First, the treatment of the boundary conditions is simpler than that used in the usual finite difference methods. Second, the finite element procedure when combined with a multistep ODE solver offers the possibility of improved accuracy in both the spatial and temporal variables as compared with the usual explicit finite difference methods.

The various methods utilized in this report for the solution of waterhammer transients are

(1) method of characteristics,
(2) Lax Method,
(3) Galerkin Method with B-splines as approximating functions,
(4) two-step Lax-Wendroff difference method,
(5) donor cell type difference method.

A complete discussion of each of the above methods will be given in subsequent sections.

## 2. GOVERNING EQUATIONS FOR WATERHAMMER TRANSIENTS

In the solution of the waterhammer problems it is assumed that the liquid is compressible and the pipe wall is extensible, but limited to an extent that the liquid density $\rho$ and the pipe diameter D do not change by more than few percent. For these conditions the bulk modulus of elasticity K of the fluid and Young's modulus E for the pipe wall are assumed to be constant. Hence, the cross sectional area A is taken as constant, but it is taken into account in that small changes in A and in $\rho$ determine the acoustic wave speed a for the system. In the case of high velocity flows with velocity varying from zero up to a, the density can change appreciably, but due to strength considerations only small changes in pipe area are permitted. In view of these assumptions, the basic governing equations can be written as

$$\frac{\partial A\rho}{\partial t} + \frac{\partial A\rho u}{\partial x} = 0 \ , \tag{2.1}$$

$$\frac{\partial A\rho u}{\partial t} + \frac{\partial A\rho u^2}{\partial x} = -A \frac{\partial p}{\partial x} - A\rho g - f \frac{\rho u|u|}{2D} A \ , \tag{2.2}$$

where A is the cross-sectional area, $\rho$, u, p are respectively, density, velocity and pressure of the fluid in the conduit, f the friction factor, D is diameter of the pipe, g is acceleration due to gravity, x is the coordinate in the axial direction, and t is the time.

From the definition of bulk modulus K, we have

$$K = \rho \frac{dp}{d\rho} \tag{2.3a}$$

or

$$K = \rho \frac{\dot{p}}{\dot{\rho}}$$

where the dot denotes total differentiation with respect to time. In terms of the pipe wall thickness b and the Young's modulus E, the rate of change of area for a thin-wall pipe is given by

$$\frac{\dot{A}}{A} = \frac{\dot{p}D}{bE} \ . \tag{2.4}$$

In terms of the piezometeric head (elevation of hydraulic grade line) H and elevation Z above the datum line, the pressure p can be expressed as

$$p = \rho_R g(H-Z) \ . \tag{2.5}$$

where $\rho_R$ is a reference density.

## 2.1 The Case of an Elastic Pipe Wall

Rewriting Eq. (2.1) as

$$\frac{\partial \rho}{\partial t} + \frac{\partial \rho u}{\partial x} + \rho \frac{\dot{A}}{A} = 0 \tag{2.6a}$$

or

$$\frac{\dot{\rho}}{\rho} + \frac{\partial u}{\partial x} + \frac{\dot{A}}{A} = 0 \ . \tag{2.6b}$$

The use of Eq. (2.4), (2.3b) and (2.5) in Eq. (2.6b) yields

$$\frac{\partial H}{\partial t} + u \frac{\partial H}{\partial x} + \frac{a^2}{g} \frac{\partial u}{\partial x} = 0 \ , \tag{2.7}$$

where a is the pressure pulse wave speed in a liquid contained in an elastic pipe and is defined by the expression

$$a = \sqrt{\frac{K/\rho_R}{1 + KD/Eb}} \tag{2.8}$$

Since density changes in waterhammer transients are relatively small, we shall therefore assume that a is essentially constant.

Rewriting Eq. (2.2) as

$$\frac{\partial \rho u}{\partial t} + \frac{\partial \rho u^2}{\partial x} + \rho u \frac{\dot{A}}{A} = - \frac{\partial p}{\partial x} - \rho g - f \frac{\rho u|u|}{2D} \tag{2.9}$$

Using Eqs. (2.6a) and (2.5) in Eq. (2.9) and assuming that the actual density is close to reference density, we obtain the equation

$$\frac{\partial u}{\partial t} + u \frac{\partial u}{\partial x} + g \frac{\partial H}{\partial x} + f \frac{u|u|}{2D} = 0 \ . \tag{2.10}$$

Equations (2.7) and (2.10) are the governing equations for unsteady flow of a liquid in an elastic pipe.

## 2.2 The Case of a Rigid Pipe Wall

In case of a pipe having a rigid wall, i.e. $\dot{A}/A = 0$ or $E \to \infty$, Eq. (2.6a) simplifies to

$$\frac{\partial \rho}{\partial t} + \frac{\partial \rho u}{\partial x} = 0 \ , \tag{2.11}$$

Eq. (2.9) reduces to

$$\frac{\partial \rho u}{\partial t} + \frac{\partial \rho u^2}{\partial x} = - \frac{\partial p}{\partial x} - \rho g - f \frac{\rho u|u|}{2D} \tag{2.12}$$

and Eqs. (2.3a) and (2.8) yield

$$a^2 = \frac{K}{\rho} = \frac{dp}{d\rho} = \rho_R \ , \tag{2.13a}$$

which for nearly constant a yields with the use of Eq. (2.5),

$$\rho = \rho_R \left[1 + g(H-H_R)/a^2\right] \tag{2.13b}$$

or

$$H = \frac{a^2}{\rho_R g} - C_R \tag{2.13c}$$

where $C_R = a^2/g - H_R$.

Equations (2.11) and (2.12) can also be written as

$$\frac{\partial \rho}{\partial t} + \frac{\partial G}{\partial x} = 0 \ , \tag{2.14}$$

$$\frac{\partial G}{\partial t} + \frac{\partial G^2/\rho}{\partial x} = - \frac{\partial p}{\partial x} - \rho g - f \frac{G|G|}{2\rho D} \ , \tag{2.15}$$

where $G = \rho u$.

It is worth noting that the system (2.7) and (2.10) is not equivalent to the system (2.14) and (2.15). To bring out the differences we proceed as follows. From Eq. (2.13c), we have

$$\rho = \rho_R g(H+c_R)/a^2 \ .$$

Thus

$$\frac{\partial \rho}{\partial t} = \frac{\rho_R g}{a^2} \frac{\partial H}{\partial t} \quad \text{and} \quad \frac{\partial \rho}{\partial x} = \frac{\rho_R g}{a^2} \frac{\partial H}{\partial x} .$$

It follows that Eq. (2.14) has the form

$$\frac{\partial H}{\partial t} + u \frac{\partial H}{\partial x} + \frac{a^2}{g} \frac{\rho}{\rho_R} \frac{\partial u}{\partial x} = 0 ,$$

which reduces to Eq. (2.7) when $\rho \equiv \rho_R$ provided the acoustic velocity a is given by Eq. (2.8). In the same way, we find that Eq. (2.15) has the form

$$\frac{\partial u}{\partial t} + u \frac{\partial u}{\partial x} + \frac{\rho_R}{\rho} g \frac{\partial H}{\partial x} + \frac{fu|u|}{2D} = 0 ,$$

which is Eq. (2.10) when $\rho \equiv \rho_R$.

## 2.3 Application to a Downstream Valve Closure Problem

The demonstration problem consists of a simple pipe system with a reservoir upstream and a valve downstream as shown in Fig. 2.1. The reservoir

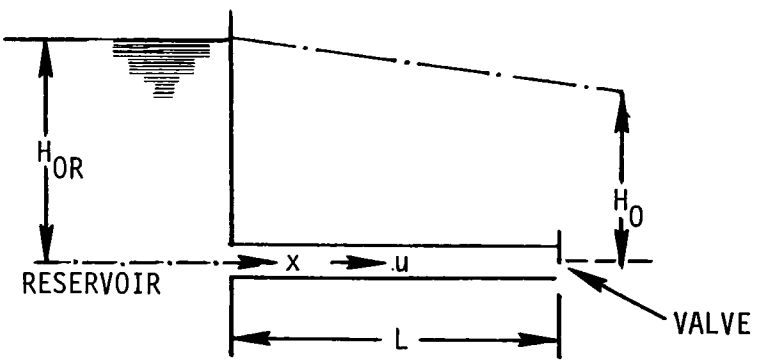


Fig. 2.1 Demonstration Problem consisting of a simple pipe system with a reservoir upstream and a valve downstream

upstream provides a relatively simple boundary condition, but the boundary condition provided by programmed valve closure at the downstream end can generate serious unsteadiness in the flow which could strain the accuracy obtainable with a given numerical scheme for the solution of the governing waterhammer equations. We assume the conditions in the pipe are steady at time t=0, and the valve then starts its prescribed motion according to

$$\tau(t) = \begin{cases} (1 - t/t_c)^m & \text{if } t < t_c \\ 0 & \text{if } t \geq t_c \end{cases}, \tag{2.16}$$

in which $t_c$ is the time of closure, m is a constant index which fixes the desired rate of closure. As is customary, the valve is treated as an orifice and consequently the discharge rate is given as

$$\frac{u_L(t)A}{u_0 A} = \frac{u_L(t)}{u_0} = \frac{C_d A_v(t)\sqrt{2gH_L(t)}}{(C_d A_v)_0\sqrt{2gH_0}} = \frac{C_d A_v(t)}{(C_d A_v)_0}\sqrt{\frac{H_L(t)}{H_0}} = \tau\sqrt{\frac{H_L(t)}{H_0}} \tag{2.17}$$

where $H_0$ is the steady-state head loss across the valve and $u_0$ is the steady-state velocity in the pipe, $C_d$ is the valve-discharge coefficient, $A_v(t)$ is the area of valve opening, subscript zero denotes the steady-state conditions, subscript L denotes the valves at the downstream end of the pipe but to the left of valve and

$$\tau = \frac{C_d A_v(t)}{(C_d A_v)_0} \quad . \tag{2.18}$$

Equation (2.17) together with Eq. (2.16) provides boundary condition at the downstream end of the pipe; the upstream boundary condition for Eqs. (2.7) and (2.10) with upstream reservoir is given

$$H(0,t) = H_{0R} \quad . \tag{2.19a}$$

The boundary condition for Eqs. (2.14) and (2.15) corresponding to the above equation is obtained by use of Eq. (2.13b) as

$$\rho(0,t) = \rho_{0R} = \rho_R\left[1 + g(H_{0R}-H_R)/a^2\right] \quad . \tag{2.19b}$$

At low velocities the steady-state solution can be given as

$$H(x) = H_{0R} - \frac{fx}{2Dg} u_0^2 \tag{2.20a}$$

or,

$$\rho(x,0) = \rho_R\left[1 + g(H(x,0)-H_R)/a^2\right] \quad . \tag{2.20b}$$

The initial condition on velocity is prescribed simply by specifying the

initial steady state flow rate as

$$u(x,0) = u_0 \ . \qquad (2.20c)$$

The specific values of various parameters used in the numerical solutions to be described in several subsequent sections are L = 4253.5 ft., a = 3963 ft./sec., D = 3 ft., f = 0.019, $u_0$ = 3.5 ft./sec., $t_c$ = 5.9 sec., $H_0$ = 300 ft., three different values of valve closure index m are chosen, namely, m = ½,1,2, $H_R$ = 300 ft. and $\rho_R$ = 62.4 $lb_m$/cu. ft.

## 3. METHOD OF CHARACTERISTICS

The nonconservative form of Eq. (2.7) and the momentum Eq. (2.10) form a pair of quasi-linear hyperbolic partial differential equations in two dependent variables, head H and velocity u; and two independent variables, distance along the pipe x and time t. The method of characteristics (MOC) is a natural choice for solving hyperbolic systems, because the governing equations are cast in a form that describes the conditions along curves called characteristics on which the physical disturbance travels.

### Characteristic Form

Following Streeter and Wylie [2] or Courant and Friedricks [3], we can proceed as follows. Let $L_1$ denote the left hand side of Eq. (2.7) and $L_2$ the left hand side of Eq. (2.10). Then we form the linear combination

$$\lambda L_1 + L_2 = \lambda\left[H_t + (g/\lambda + u)H_x\right] + \left[u_t + \left(u + \frac{\lambda a^2}{g}\right)u_x\right] + \frac{u|u|f}{2D} = 0 \ . \quad (3.1)$$

Choose $\lambda$ so that each expression in the brackets is a directional derivative in the same direction. That is,

$$u_t + \left(u + \frac{\lambda a^2}{g}\right)u_x = \frac{du}{dt} = u_t + \frac{dx}{dt}\,u_x \ , \text{ and}$$

$$H_t + (g/\lambda + u)H_x = \frac{dH}{dt} = H_t + \frac{dx}{dt}\,H_x \text{ on the curve } x = x(t) \ .$$

Then

$$\frac{dx}{dt} = u + \frac{\lambda a^2}{g} = u + g/\lambda \ ,$$

which gives

$$\lambda = \pm g/a \ , \quad (3.2)$$

and the equations for the characteristics

$$\frac{dx}{dt} = u \pm a \ . \quad (3.3)$$

Let $C^+(C^-)$ denote the characteristic curve defined by the +(-) sign in Eq. (3.3). Using Eq. (3.2) in Eq. (3.1), we obtain the following pairs of equations.

$$\left.\begin{aligned} &\text{a)}\quad \frac{dx}{dt} = u+a \\ &\text{b)}\quad \frac{g}{a}\frac{dH}{dt} + \frac{du}{dt} + \frac{u|u|f}{2D} = 0 \end{aligned}\right\} \text{ on } C^+ \tag{3.4}$$

$$\left.\begin{aligned} &\text{a)}\quad -g/a\,\frac{dH}{dt} + \frac{du}{dt} + \frac{u|u|f}{2D} = 0 \\ &\text{b)}\quad \frac{dx}{dt} = u-a \end{aligned}\right\} \text{ on } C^- \tag{3.5}$$

Method of Characteristics

In the method of characteristics, the numerical procedure starts with the above system of ordinary differential equations. Suppose that at time $t = t_0$, we know $H(x,t_0)$ and $u(x,t_0)$ for all $0 \le x \le L$, and consider the problem of determining $H(x,t_1)$ and $u(x,t_1)$ for some $t_1 > t_0$. Let P be any point on the line $t = t_1$; then the characteristic curve $C^+$ through P will intersect the time $t = t_0$ at R and $C^-$ will intersect the line $t = t_0$ at S as shown in Fig. 3.1.

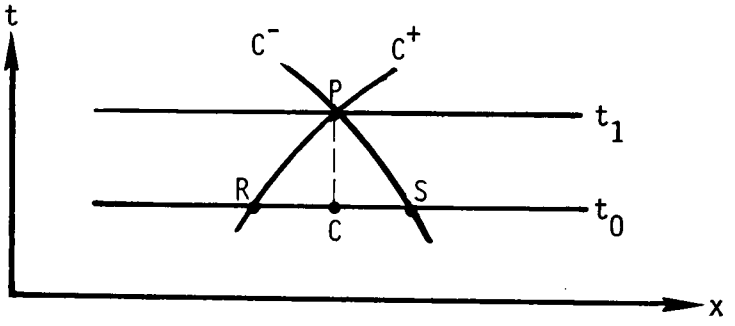


Fig. 3.1 Display of the Characteristics

Let $x^{\pm}(t)$ denote the function defining the curve $C^{\pm}$, and set

$$H^{\pm}(t) = H(x^{\pm}(t),t),\ u^{\pm}(t) = u(x^{\pm}(t),t),$$
$$x_R = x^+(t_0),\ x_S = x^-(t_0),\ x_P = x_C = x^+(t_1) = x^-(t_1),$$
$$H_R = H(x_R,t_0),\ H_S = H(x_S,t_0),\ u_R = u(x_R,t_0),\ u_S = u(x_S,t_0).$$

With this notation, the system (3.4) and (3.5) has the form:

$$\text{a)}\quad \frac{dx^+}{dt} = u^+(t)+a$$
$$\text{b)}\quad \frac{g}{a}\frac{dH^+}{dt} + \frac{du^+}{dt} + \frac{u^+|u^+|f}{2D} = 0 \qquad (3.6)$$

$$\text{a)}\quad -\frac{g}{a}\frac{dH^-}{dt} + \frac{du^-}{dt} + \frac{u^-|u^-|f}{2D} = 0$$
$$\text{b)}\quad \frac{dx^-}{dt} = u^-(t)-a \qquad (3.7)$$

This system in turn is equivalent to the following system of integral equations.

$$\text{(i)}\quad x_p - x_R = \int_{t_0}^{t_1}(u^+(t)+a)dt$$
$$\text{(ii)}\quad (g/a)H_p + u_p = (g/a)H_R + u_R - \frac{f}{2D}\int_{t_0}^{t_1}u^+(t)|u^+(t)|dt = \sigma_1$$
$$\text{(iii)}\quad -(g/a)H_p + u_p = -(g/a)H_s + u_s - \frac{f}{2D}\int_{t_0}^{t_1}u^-(t)|u^-(t)|dt = \sigma_2 \qquad (3.8)$$
$$\text{(iv)}\quad x_p - x_s = \int_{t_0}^{t_1}(u^-(t)-a)dt$$

From the 2nd and 3rd equation of the system, we find

$$\text{a)}\quad H(x_p,t_1) = H_p = \frac{a}{2g}(\sigma_1-\sigma_2)$$
$$\text{b)}\quad u(x_p,t_1) = u_p = \frac{1}{2}(\sigma_1+\sigma_2) \qquad (3.9)$$

Approximate Equations

Up to this point no approximation has been made in deriving the system (3.8) and (3.9). There are two separate approximations which have to be made in the system (3.8). The first involves an approximation of the integrals appearing in (3.8). The nature of this approximation determines whether the resulting scheme is explicit or implicit, single time step or multistep. The second approximation involves the data on the base line $t = t_0$ which is discrete in nature; therefore, in general, the values $H_R$, $u_R$, $H_s$, $u_s$ must be approximated by an interpolatory scheme of some type.

The following approximation is used in evaluating the integrals

$$\left.\begin{aligned} u^{+}(t) &\cong u_R \ , \\ u^{-}(t) &\cong u_s \ , \end{aligned}\right\} \quad t_0 \le t \le t_1 \ . \tag{3.10}$$

This approximation leads to the following explicit single step scheme.

$$\begin{aligned} &\text{(i)} \quad x_p - x_R = \delta t(u_R+a) \\ &\text{(ii)} \quad x_p - x_s = \delta t(u_s-a) \\ &\text{(iii)} \quad \sigma_1 = (g/a)H_R + u_R - \frac{\delta t f}{2D} u_R|u_R| \\ &\text{(iv)} \quad \sigma_2 = (-g/a)H_s + u_s - \frac{\delta t f}{2D} u_s|u_s| \\ &\text{(v)} \quad H_p = \frac{a}{2g}(\sigma_1-\sigma_2) \\ &\text{(vi)} \quad u_p = \frac{1}{2}(\sigma_1+\sigma_2) \end{aligned} \tag{3.11}$$

Boundary Conditions

Before discussing interpolation schemes for the initial data, we complete the discussion of determining $H(x,t_1)$ and $u(x,t_1)$ by considering the boundaries. At the left boundary, only the $C^-$ characteristic carries information from the base line $t = t_0$. Equations (3.8 iii-iv) are associated with the $C^-$ curve; hence when approximation (3.10) is used, we obtain:

$$\begin{aligned} &\text{a)} \quad x_p - x_s = \delta t(u_s-a) \ , \\ &\text{b)} \quad (-g/a)H_p + u_p = (-g/a)H_s + u_s - \frac{f}{2D} u_s|u_s| = \sigma_2 \ . \end{aligned} \tag{3.12}$$

Now the boundary condition (2.19) applies at the left, and when used in Eq. (3.12) yields:

$$u_p = (g/a)H_{OR} + \sigma_2 \ , \tag{3.13}$$

where $\sigma_2$ is defined in (3.12a).

On the right boundary, only the $C^+$ characteristic intersects the domain; hence when approximation (3.10) is used in conjunction with (3.8 i-ii), we find

$$\begin{aligned} &\text{a)} \quad x_p - x_R = \delta t(u_R + a) \\ &\text{b)} \quad (g/a)H_p + u_p = (g/a)H_R + u_R - \frac{f}{2D} u_R|u_R| = \sigma_1 \ . \end{aligned} \tag{3.14}$$

In the present notation, the boundary condition (2.17) on the right takes the form

$$u_p = \tau u_0 \sqrt{H_p/H_0} \ . \tag{3.15}$$

Let $\beta = \sqrt{H_p/H_0}$, then $\beta \geq 0$, and from Eqs. (3.15) and (3.14b), we find

$$\frac{gH_0}{a} \beta^2 + \tau u_0 \beta - \sigma_1 = 0 \ , \tag{3.16}$$

which has the unique non-negative root ($\sigma_1 \geq 0$ from Eq. (3.14b))

$$\beta = \left(-\tau u_0 + \sqrt{\tau^2 u_0^2 + 4\sigma_1 g H_0/a}\right) \Big/ (2gH_0/a) \ . \tag{3.17}$$

Hence

$$\begin{aligned} &\text{a)} \quad H_p = H_0 \beta^2 \ , \\ &\text{b)} \quad u_p = \tau u_0 \beta \ . \end{aligned} \tag{3.18}$$

When the initial data is given, then Eqs. (3.13), (3.11), and (3.18) constitute an explicit single step scheme for determining $H(x,t_1)$, and $u(x,t_1)$.

Interpolation

We now consider the second approximation which involves the problem of representing the data at $t = t_0$. To this end we construct an equally spaced

grid on the interval [0,L] by setting

$$\text{a)} \quad \delta x = L/N, \text{ and}$$
$$\text{b)} \quad x_i = (i-1)\delta x, \quad \text{for} \quad i=1,2,\ldots,N+1 , \tag{3.19}$$

where N is a given integer. Assume that at $t = t_n$ the initial data is known at the grid points $x_i$, and write $H_i^n = H(x_i,t_n)$, $u_i^n = u(x_i,t_n)$. Consider a portion of the grid as shown in Fig. 3.2.

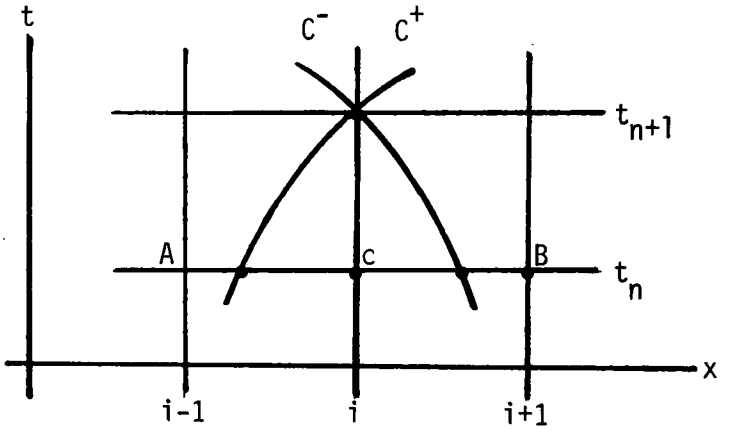


Fig. 3.2 A Portion of the Grid in the x-t Plane

Let W denote either of the dependent variables H or u, and set $W_A = W_{i-1}^n$, $W_B = W_{i+1}^n$, $W_C = W_i^n$. Then $W_A$, $W_B$, $W_C$ are known and the problem is to determine $W_R = W(x_R,t_n)$ and $W_S = W(x_S,t_n)$. In order to ensure that the points $X_R$ and $X_S$ are in the interval $[X_A,X_B]$, it is necessary to restrict the time step $\delta t_n = t_{n+1}-t_n$. From Eqs. (3.11 i-ii), we see that the following condition will suffice

$$\delta t_n \leq \delta x/(\bar{u}^n+a) , \tag{3.20}$$

where $\bar{u}^n = \max\{|u_i^n|: 1 \leq i \leq N+1\}$. In practice, the equality sign is used in (3.20).

The approximation (3.10) generates an error of order $O(\delta t^2)$ in the integrals appearing in Eqs. (3.8). It would be natural then to consider interpolation schemes of comparable accuracy. Linear interpolation is such a scheme,

and we present first the linear interpolation scheme. We shall also present a quadratic interpolation scheme; although we will not consider a corresponding higher order approximation for Eq. (3.10).

Linear Interpolation

Consider the interpolation of u. From Fig. 3.2, we find

$$\text{a)}\quad u_R = (|RC|u_A + |AR|u_c)/\delta x \ ,$$
$$\text{b)}\quad u_s = (|Cs|u_B + |sB|u_c)/\delta x \ . \tag{3.21}$$

From Eqs. (3.11 i-ii), we find

$$|RC| = x_p - x_R = \delta t(u_R+a) \ ,$$
$$|AR| = \delta x - \delta t(u_R+a) \ ,$$
$$|Cs| = x_s - x_p = \delta t(a-u_s) \ ,$$
$$|sB| = \delta x - \delta t(a-u_s) \ ;$$

thus setting $\alpha = \delta t/\delta x$, we have

$$\text{a)}\quad u_R = \left[u_C + \alpha a(u_A-u_C)\right]\Big/\left[1 + \alpha(u_C-u_A)\right] \ ,$$
$$\text{b)}\quad u_s = \left[u_C + \alpha a(u_B-u_C)\right]\Big/\left[1 + \alpha(u_B-u_C)\right] \ . \tag{3.22}$$

With $u_R$ and $u_s$ determined, the linear interpolation for $H_R$ and $H_s$ are given by

$$\text{a)}\quad H_R = (|RC|H_A + |AR|H_C)/\delta x$$
$$= \alpha(a+u_R)H_A + \left[1 - \alpha(a+u_R)\right]H_C \ , \tag{3.23}$$
$$\text{b)}\quad H_s = \alpha(a-u_s)H_B + \left[1 - \alpha(a-u_s)\right]H_C \ .$$

With the interpolation of the data at $t = t_n$ as given above, the method of characteristic procedure described herein is complete. Two approximations were involved, the first in (3.10) and the second in the use of linear

interpolation. The resulting scheme is an explicit single time step procedure.

Quadratic Interpolation

For quadratic interpolation we set $\sigma = (x-x_C)/\delta x$, and we assume

$$W = A_1\sigma^2 + A_2\sigma + W_C \ , \tag{3.24}$$

where

$$\begin{aligned} &a) \quad A_1 = (W_B-2W_C+W_A)/2 \ , \\ &b) \quad A_2 = (W_B-W_A)/2 \ , \end{aligned} \tag{3.25}$$

and W denotes either u or H. We first consider the interpolation of u at $x_R$, then $\sigma_R = (x_R-x_C)/\delta x = -\alpha(a+u_R)$, and

$$u_R = A_1\alpha^2(a+u_R)^2 - A_2\alpha(a+u_R) + u_C \tag{3.26}$$

or

$$A_1\alpha^2u_R^2 + \left[2A_1a\alpha^2-A_2\alpha-1\right]u_R + A_1a^2\alpha^2 - A_2a\alpha + u_C = 0 \tag{3.27}$$

where $A_1, A_2$ are defined in (3.25) with W = u.

The discriminant of this equation is

$$D(\alpha) = \left[A_2^2 - 4A_1(a+u_C)\right]\alpha^2 + 2A_2\alpha + 1 \ . \tag{3.28}$$

Recall that $\alpha_0 = \delta t/\delta x = \dfrac{1}{a + |\bar{u}|}$ where $|\bar{u}| = \max|u_i|$, $a >> |\bar{u}|$, and from (3.25), $|A_1| \leq 2|\bar{u}|$, $|A_2| \leq |\bar{u}|$; thus it is not difficult to show that $D(\alpha_0) > 0$. That is Eq. (3.27) has real roots for $\alpha = \alpha_0$.

If we set

$$E_1 = A_1\alpha^2 ,$$
$$E_2 = 2A_1a\alpha^2 - A_2\alpha - 1 , \tag{3.29}$$
$$E_3 = A_1a^2\alpha^2 - A_2a\alpha + u_C ,$$

then Eq. (3.25) has the two roots

$$u_R^{(1)} = -2E_3/(E_2-\sqrt{D}) ,$$
$$U_R^{(2)} = -2E_3/(E_2+\sqrt{D}) . \tag{3.30}$$

Since $\alpha = \dfrac{1}{a + |\bar{u}|}$ and $a >> |\bar{u}|$, it follows that $E_2 < 0$; thus

$$u_R^{(1)} = 2E_3/(|E_2|+\sqrt{D})$$
$$u_R^{(2)} = 2E_3/(|E_2|-\sqrt{D}) \tag{3.31}$$

We must now decide which root to select. Since $\alpha = 1/(a+|\bar{u}|)$ and $a >> |\bar{u}|$we know that $\alpha << 1$; but then for small $\alpha$ we have

$$|E_2| - \sqrt{D} \doteq (\tfrac{1}{2}A_2^2+2A_1u_C)\alpha^2 + O(\alpha^3) ;$$

whereas

$$|E_2| + \sqrt{D} \doteq 2\left[1+A_2\alpha+O(\alpha^2)\right] .$$

Thus for $\alpha$ small, the root $u_R^{(2)}$ is extraneous, and $u_R^{(1)}$ is the proper choice for $u_R$. We also note that if $A_1 = 0$ (u is linear), then $u_R^{(1)}$ gives the correct linear interpolation with a stable computational expression.

Having determined $u_R$, the quadratic interpolant $H_R$ follows from Eq. (3.24).

$$H_R = H_C - B_2\alpha(a+u_R) + B_1(\alpha(a+u_R))^2 .$$

The procedure for determining $u_s$ and $H_s$ is similar to the task of determining $u_R$ and $H_R$. In this case $\sigma = (x_s - x_c)\delta x = \alpha(a-u_s)$, and $u_s$ satisfies

$$A_1\alpha^2 u_s^2 + (-2A_1 a\alpha^2 - A_2\alpha - 1)u_s + A_1 a^2\alpha^2 + A_2 a\alpha + u_c = 0 \ . \tag{3.33}$$

If we set

$$\begin{aligned} \tilde{E}_1 &= A_1\alpha^2 \ , \\ \tilde{E}_2 &= -2A_1 a\alpha^2 - A_2\alpha - 1 \ , \\ \tilde{E}_3 &= A_1 a^2\alpha^2 + A_2 a\alpha + u_c \\ \tilde{D} &= (\tilde{E}_2)^2 - 4\tilde{E}_1\tilde{E}_3 = \left[A_2^2 + 4A_1(a-u_c)\right]\alpha^2 + 2A_2\alpha + 1 \ , \end{aligned} \tag{3.34}$$

then as before $\tilde{E}_2 < 0$ and $\tilde{D} > 0$ for $\alpha = 1/(a+|\bar{u}|)$, and the interpolants are

$$\begin{aligned} &\text{a)} \quad u_s^{(1)} = 2\tilde{E}_3/(|\tilde{E}_2| + \sqrt{\tilde{D}}) \\ &\text{b)} \quad H_s = H_c + B_2\alpha(a-u_s) + B_1(\alpha(a-u_s))^2 \ . \end{aligned} \tag{3.35}$$

Truncation Error and Stability

Computational experience has shown that when the criterion (3.20) is used to select the time steps, the method of characteristics presented herein is computationally stable. Moreover, the use of characteristics leads directly to the concept of a domain of influence which is central in the development of the Courant, Friedrick, Lewy condition for the linear wave equation [4]. In this report, we intend to investigate some aspects of the computational stability associated with each method discussed. The investigation will be based on an application of the heuristic stability theory developed by Hirt [5]. This theory is not only heuristic and incomplete, but it is also restricted to considering the treatment at interior points while ignoring all aspects of boundary conditions and their relation to stability. Nevertheless, the approach is applicable to nonlinear equations, and it can provide some insight for some aspects of computational stability.

Since this investigation involves the use of Hirt's stability theory, we refer the interested reader to his paper [5] for a complete discussion. It

will suffice at this point to summarize the basic ideas. The first step is to reduce the discrete equation (e.g. finite difference equation) to a differential equation by expanding each term in a Taylor series. For a consistent approximation, the lowest order terms in the expansion must represent the original differential equation. The higher order terms are the truncation errors. In Hirt's approach, stability is investigated by examining the lowest order truncation errors. In particular, the lowest order truncation error terms usually turn out to constitute a wave equation. Its domain of influence is then compared with the domain of influence of the discrete equation. Some stability criteria are then inferred on the basis of requiring that the domain of influence for the discrete equation include the domain of influence for the wave equation. The lowest order truncation errors are then rewritten in such a way that the original equation together with the lowest order truncation error forms a parabolic equation. Additional stability criteria are then inferred by requiring that the parabolic equation is mathematically stable. A single parabolic equation $y_t = Dy_{xx}$ would be mathematically stable if $D > 0$. In the present application we are dealing with a system of two equations; thus a parabolic type equation would have the form $W_t = DW_{xx}$ where $W = (W^1, W^2)'$ and $D = \begin{pmatrix} D_{11} & D_{12} \\ D_{21} & D_{22} \end{pmatrix}$. If P is a similarity matrix such that $PDP^T = \mathrm{diag}(\lambda_1, \lambda_2)$ or possibly $PDP^T = \begin{pmatrix} \lambda & 1 \\ 0 & \lambda \end{pmatrix}$ then setting $\phi = PW$ implies that the system $W_t = DW_{xx}$ is equivalent to

$$\phi^1_t = \lambda_1 \phi^1_{xx} ,$$

$$\phi^2_t = \lambda_2 \phi^2_{xx} ;$$

or

$$\phi^1_t = \lambda \phi^1_{xx} + \phi^2_{xx} ,$$

$$\phi^2_t = \lambda \phi^2_{xx} .$$

In either case, it is clear that the system $W_t = DW_{xx}$ is mathematically stable if the matrix D has a real, positive spectrum. For this we have the following criteria:

a) $\lambda_i$ real iff $(D_{11}-D_{22})^2 + 4D_{12}D_{21} > 0$.

b) $\lambda_i$ real if $D_{12}$ and $D_{21}$ have the same sign. (3.36)

c) If $\lambda_i$ real, then $\lambda_i$ is non-negative when $D_{11}D_{22}-D_{12}D_{21} \geq 0$ .

We shall apply the Hirt technique to the method of characteristics in the case when linear interpolation was used. We start with Eq. (3.22) for $u_R$ and $u_s$ expanding these expressions in a Taylor series about a typical interior mesh point $x_i$. For notational simplicity, we write $u = u_i$, $u_x = (u_x)_i$, etc. Then

$$u_R = \frac{u_i + \alpha a(u_{i-1}-u_i)}{1 + \alpha(u_i-u_{i-1})}$$

$$= u + \delta t\left[-(a+u)u_x+\tfrac{1}{2}(a+u)\delta x u_{xx}\right] + \delta t^2\left[au_x^2-a\delta x u_x u_{xx}\right] + O(\delta x^2,\delta t^3) \quad (3.37)$$

$$u_s = \frac{u_i + \alpha a(u_{i+1}-u_i)}{1 + \alpha(u_{i+1}-u_i)}$$

$$= u + \delta t\left[(a-u)u_x+(a-u)\frac{\delta x}{2}u_{xx}\right] + \delta t^2\left[-au_x^2-a\delta x u_x u_{xx}\right] + O(\delta t^3,\delta x^2) \quad (3.38)$$

With these expansions and Eq. (3.23), we have the following expansions for $H_R$ and $H_s$.

$$H_R = H_i + \alpha(a+u_R)(H_{i-1}-H_i)$$

$$= H + \delta t(a+u)\left[-H_x + \frac{\delta x}{2}H_{xx}\right] + \delta t^2\left[(a+u)H_x u_x - \frac{\delta x}{2}(a+u)(u_x H_{xx}+H_x u_{xx})\right] + O(\delta t^3,\delta x^2) \quad (3.39)$$

$$H_s = H_i + \alpha(a-u_s)(H_{i+1}-H_i)$$
$$= H + \delta t(a-u)\left[H_x + \frac{\delta x}{2} H_{xx}\right] - \delta t^2\left[(a-u)u_x H_x + \frac{\delta x}{2}(a-u)(u_x H_{xx}+H_x u_{xx})\right] \tag{3.40}$$
$$+ O(\delta t^3, \delta x^2)$$

Now

$$\text{a)} \quad H_i^{n+1} = H + \delta t H_t + \frac{\delta t^2}{2} H_{tt} + O(\delta t^3) ,$$
$$\text{b)} \quad u_i^{n+1} = u + \delta t u_t + \frac{\delta t^2}{2} u_{tt} + O(\delta t^3) ; \tag{3.41}$$

thus, if we use the above expansions in Eqs. (2.11, iii-vi), we find, after some algebra,

$$H_t + uH_x + \frac{a^2}{g} u_x = -\frac{\delta t}{2} H_{tt} + \frac{a\delta x}{2} H_{xx} + \frac{au}{2g}\delta x\, u_{xx}$$
$$+ \delta t u_x H_x + \delta t \frac{a^2}{g}\left(u_x + \frac{f}{D}\right)u_x + O(\delta t \delta x, \delta t^2, \delta x^2) \tag{3.42}$$

$$u_t + uu_x + gH_x + \frac{fu|u|}{2D} = -\frac{\delta t}{2} u_{tt} + \frac{\delta x}{2}\frac{gu}{a} H_{xx} + \frac{a\delta x}{2} u_{xx}$$
$$+ \delta t g H_x u_x - \frac{\delta t f u u_x}{D} + O(\delta t \delta x, \delta t^2, \delta x^2) . \tag{3.43}$$

If we ignore the higher order truncation error terms in Eqs. (3.42) and (3.43), we have a pair of second order partial differential equations. We assert that this is a hyperbolic system, and by comparing its domain of influence with the domain of influence of the discrete system (3.11), we will find the first stability criterion. To find the characteristics of this system, we write the system (3.42 - 3.43) in the form

$$\text{a)} \quad -H_{tt} + aH_{xx} + \frac{au}{g} u_{xx} + \ldots = 0$$
$$\text{b)} \quad -u_{tt} + au_{xx} + \frac{ug}{a} H_{xx} + \ldots = 0 . \tag{3.44}$$

Next we write this as a system of first order equations. To this end, set $\phi^1 = H_t$, $\phi^2 = H_x$, $\phi^3 = u_t$, $\phi^4 = u_x$, then (2.44) has the form:

$$A\phi_t + B\phi_x + \ldots = 0$$

where

$$A = \mathrm{diag}[-\alpha, 1, -\alpha, 1]$$

$$B = \begin{bmatrix} 0 & a & 0 & au/g \\ -1 & 0 & 0 & 0 \\ 0 & ug/a & 0 & a \\ 0 & 0 & -1 & 0 \end{bmatrix} \tag{3.46}$$

The roots of $\det[B-\lambda A] = 0$ will then determine the characteristic directions for the system (3.45). Now

$$\det[B-\lambda A] = \alpha^2\lambda^4 - 2a\alpha\lambda^2 + a^2 - u^2 = 0 \; ; \tag{3.47}$$

hence

$$\lambda^2 = \frac{a \pm |u|}{\alpha} \; . \tag{3.48}$$

Since $a > |u|$, we are assured that all roots are real and distinct; hence the system is hyperbolic, and the four roots are

$$\lambda = \pm \sqrt{\frac{a \pm |u|}{\alpha}} \; . \tag{3.49}$$

Now the characteristic directions are determined by the differential equations

$$\frac{dx}{dt} = \lambda \; , \tag{3.50}$$

where $\lambda$ is any one of the four values defined in (3.49). If the discrete equation (3.11) is to have solutions approximating the solutions of the hyperbolic system (3.44), then its domain of influence must include the domain of influence of (3.46). That is

$$|\lambda| = \left|\frac{dx}{dt}\right| \leq \frac{1}{\alpha} \; , \tag{3.51}$$

or

$$\lambda^2 = \frac{a \pm |u|}{\alpha} < \frac{1}{\alpha^2} ,$$

i.e.

$$\alpha \leq \frac{1}{a \pm |u|} .$$

Since $a-|u| < a+|u|$, this is the usual Courant, Friedricks, Lewy condition and is the same as condition (3.10).

In accordance with the Hirt approach, we now look for a second stability criterion by rewriting Eqs. (3.42) and (3.43). This is accomplished by expressing $H_{tt}$ and $u_{tt}$ in terms of partial derivatives in x by using the original differential equations. Thus

$$H_{tt} = u_t H_x - u H_{xt} - a^2/g\, u_{xt} \tag{3.52}$$
$$= (u^2+a^2) H_{xx} + \frac{2a^2 u}{g} u_{xx} + \dots ,$$

$$u_{tt} = -u_x u_t - u u_{xt} - g H_{xt} - \frac{f u u_x}{D} \tag{3.53}$$
$$= 2ugH_{xx} + (u^2+a^2) u_{xx} + \dots .$$

When these expressions are used in (3.42) and (3.43) we obtain the following expressions.

$$\text{a)} \quad H_t + uH_x + \frac{a^2}{g} u_x = \frac{a\delta x}{2} - \frac{\delta t}{2} (a^2+u^2) H_{xx} + \frac{au}{2g} (\delta x - 2a\delta t) u_{xx} + \dots$$

$$\text{b)} \quad u_t + u u_x + g H_x + \frac{f u |u|}{2D} = \frac{ug}{2a} (\delta x - 2a\delta t) H_{xx} + \frac{a\delta x}{2} - \frac{\delta t}{2} (a^2+u^2) u_{xx} + \dots \tag{3.54}$$

Here, to lowest order terms, we have a parabolic system, and in order to have a mathematically stable system, the diffusion matrix should have real, positive spectrum. In the notation of (3.36), we have

$$D_{11} = D_{22} = \frac{\delta x}{2} (a - \alpha(a^2+u^2)) ,$$

$$D_{12} = \frac{au\delta x}{2g} (1-2a\alpha), \quad D_{21} = \frac{ug\delta x}{2a} (1-2a\alpha) . \tag{3.55}$$

We first observe that the spectrum is always real, since

$$(D_{11}-D_{22})^2 + 4D_{12}D_{21} = u^2\delta x^2(1-2a\alpha)^2 > 0 .$$

Referring to Eq. (3.36c) we observe

$$\begin{aligned} D_{11}D_{22}-D_{12}D_{21} &= \frac{\delta x^2}{4}\left[(a - \alpha(a^2+u^2))^2 - u^2(1-2a\alpha)^2\right] \\ &= \frac{\delta x^2}{4}(a^2-u^2)\left[1 - \alpha(a+u)\right]\left[1 - \alpha(a-u)\right] \geq 0 . \end{aligned}$$

If both of the last two factors were negative, then the first stability criterion would be violated; hence both must be non-negative in which case we obtain the first stability criterion.

In summary, the Hirt analysis provides us with a plausible stability criterion for the characteristic method. Although this criterion is almost self evident in the case of a characteristic method, this exercise does provide the confidence and technique for use on other approximations.

## 4. LAX METHOD

The Lax finite difference method (cf. Lax [6], Roache [7], Potter [8]) is a single step, explicit method which is applicable to the water hammer equations.

We subdivide the interval [0,L] into N equal subintervals of length $\delta x = L/N$ with the mesh $x_i = (i-1)\delta x$ for $1 \le i \le N+1$. Again, we identify $H_i^n = H(x_i,t_n)$ and $u_i^n = u(x_i,t_n)$ where $t_n = \sum_{k=0}^{n-1} \delta t_k$ with $\delta t_n$ determined by the Courant condition

$$\delta t_n \le \frac{\delta x}{a + \bar{u}^n}, \quad \bar{u}^n = \max\{|u_i^n|: 1 \le i \le N+1\} . \tag{4.1}$$

In practice we select the equality sign.

### Difference Equations

The Lax difference method uses central spatial differences and single forward time difference but with a spatial average replacing the pivot value. At the interior points $x_j$, $2 \le j \le N$, the Lax difference equations for the water hammer Eqs. (2.7) and (2.10) are as follows.

$$\text{a)} \quad H_j^{n+1} = \tfrac{1}{2}(H_{j-1}^n + H_{j+1}^n) - \tfrac{\alpha}{2}\left[u_j^n(H_{j+1}^n - H_{j-1}^n) + \frac{a^2}{g}(u_{j+1}^n - u_{j-1}^n)\right] ,$$

$$\text{b)} \quad u_j^{n+1} = \tfrac{1}{2}(u_{j-1}^n + u_{j+1}^n) - \tfrac{\alpha}{2}\left[u_j^n(u_{j+1}^n - u_{j-1}^n) + g(H_{j+1}^n - H_{j-1}^n)\right] \tag{4.2}$$

$$- \delta t\, u_j^n |u_j^n| f/2D ,$$

where, as usual, $\alpha = \delta t/\delta x$.

### Boundary Conditions

At the left boundary, the head is specified by Eq. (2.19); thus an equation for determining $u_1^{n+1}$ is needed. Since the Lax method involves central spatial differences, it is not directly applicable at the boundary; hence some other approach will have to be used. Here we use a single step, one sided spatial difference approximation to the momentum Eq. (2.10).

$$u_1^{n+1} = u_1^n - \alpha\left[u_1^n(u_2^n-u_1^n) + g(H_2^n-H_1^n)\right] - \delta t\, u_1^n|u_1^n|f/2D\ , \tag{4.3}$$

together with the boundary condition (2.19)

$$H_1^{n+1} = H_{0R}\ . \tag{4.4}$$

We next consider the right boundary. Equation (2.17), in the current notation, has the form

$$u_{N+1}^{n+1} = u_0\tau^{n+1}\sqrt{H_{N+1}^{n+1}/H_0}\ . \tag{4.5}$$

Again, the Lax method is not directly applicable; so we use a single step, one sided difference approximation to the momentum Eq. (2.10)

$$\begin{aligned} u_{N+1}^{n+1} = u_{N+1}^n &- \alpha\left[u_{N+1}^n(u_{N+1}^n-u_N^n) + g(H_{N+1}^{n+1}-H_N^{n+1})\right] \\ &- \delta t\, u_{N+1}^n|u_{N+1}^n|f/2D\ . \end{aligned} \tag{4.6}$$

Note that this equation is implicit since we have used $H_{N+1}^{n+1}-H_N^{n+1}$ on the right side. As a consequence, Eqs. (4.5) and (4.6) must be solved simultaneously. Before solving this system we shall make a few comments. First, numerical experience has convinced us that an explicit procedure at this boundary will not be stable. For example, if an explicit version of (4.6) is used to determine $u_{N+1}^{n+1}$ and if (4.5) is then used to determine $H_{N+1}^{n+1}$, the resulting scheme is unstable for $\delta t_n = \gamma(\delta t_n)_0$, $0.1 \le \gamma \le 1$, where $(\delta t_n)_0$ is given by Eq. (4.1) with the equality sign. The second remark is that since the difference scheme is explicit at the left boundary and the interior points, it is not necessary to use a more elaborate implicit scheme than the one used in (4.6).

To solve the system (4.5) and (4.6), we set $\beta = \sqrt{H_{N+1}^{n+1}/H_0}$; then from Eq. (4.5) we have $u_{N+1}^{n+1} = u_0\tau\beta$, and using this in Eq. (4.6), we find that $\beta$ satisfies $A_1\beta^2 + A_2\beta - A_3 = 0$, where

$$\begin{aligned} &\text{a)}\quad A_1 = \alpha g H_0 \\ &\text{b)}\quad A_2 = u_0\tau \\ &\text{c)}\quad A_3 = u_{N+1}^n - \alpha\left[u_{N+1}^n(u_{N+1}^n-u_N^n) - gH_N^{n+1}\right] - \delta t f u_{N+1}^n|u_{N+1}^n|/2D\ . \end{aligned} \tag{4.7}$$

Since $\beta$ is positive, we select the positive root

$$\beta = \left[-u_0\tau + \sqrt{(u_0\tau)^2 + 4\alpha g H_0 A_3}\right]/2\alpha g H_0 \ , \tag{4.8}$$

and

$$\begin{aligned} &\text{a)} \quad H_{N+1}^{n+1} = H_0\beta^2 \ , \\ &\text{b)} \quad u_{N+1}^{n+1} = u_0\tau\beta \ . \end{aligned} \tag{4.9}$$

Truncation Error and Stability

Expanding Eqs. (4.2) in a Taylor series, and retaining the lowest order terms in the truncation error, we obtain

$$\begin{aligned} &\text{a)} \quad H_t + uH_x + \frac{a^2}{g}u_x = -\frac{\delta t}{2}H_{tt} + \frac{\delta x^2}{2\delta t}H_{xx} - \frac{\delta x^2}{6}uH_{xxx} - \frac{a^2}{g}\frac{\delta x^2}{6}u_{xxx} \\ &\qquad\qquad + C(\delta t^2, \delta x^4/\delta t^2, \delta x^3) \\ &\text{b)} \quad u_t + uu_x + gH_x + \frac{fu|u|}{2D} = -\frac{\delta t}{2}u_{tt} + \frac{\delta x^2}{2\delta t}u_{xx} - \frac{\delta x^2}{6}uu_{xxx} \\ &\qquad\qquad - \frac{\delta x^2}{6}gH_{xxx} + O(\delta t^2, \delta x^4/\delta t^2, \delta x^3) \ . \end{aligned} \tag{4.10}$$

Assuming that we can neglect the terms involving third order derivatives, we find that we have a pair of second order hyperbolic equations which are not coupled in the second order terms. For each equation, the characteristics are defined by

$$\frac{dx}{dt} = \pm\frac{\delta x}{\delta t} \ ,$$

hence the domain of influence of the difference equation is the same as the domain of influence of the system (4.10). In this situation, no restriction is imposed on $\alpha$. We look for the second stability criterion by using the expansions (3.52) and (3.53) in the lowest order terms. We find

$$\begin{aligned} &\text{a)} \quad H_t + uH_x + \frac{a^2}{g}u_x = \left[\frac{\delta x^2}{2\delta t} - \frac{\delta t}{2}(a^2+u^2)\right]H_{xx} - \left[\frac{\delta t a^2 u}{g}\right]u_{xx} + \ldots \\ &\text{b)} \quad u_t + uu_x + gH_x + \frac{fu|u|}{2D} = -\delta t g u H_{xx} + \left[\frac{\delta x^2}{2\delta t} - \frac{\delta t}{2}(a^2+u^2)\right]u_{xx} + \ldots \end{aligned} \tag{4.11}$$

Thus we have the following diffusion matrix coefficients

$$D_{11} = D_{22} = \frac{\delta t}{2}\left[\frac{1}{\alpha^2} - (a^2+u^2)\right] ,$$

$$D_{12} = -\frac{\delta t a^2 u}{g}, \quad D_{21} = -\delta t g u .$$

Referring to the criteria in (3.36), we observe that since $D_{12}$ and $D_{21}$ have the same sign, the spectrum of D is always real. In order for the spectrum to be non-negative, we must have

$$D_{11}D_{22} - D_{12}D_{21} = \frac{\delta t^2}{4}\left[\frac{1}{\alpha^2} - (a+u)^2\right]\left[\frac{1}{\alpha^2} - (a-u)^2\right] \geq 0 ,$$

i.e. the usual Courant condition

$$\alpha \leq \frac{1}{a + |u|} . \tag{4.12}$$

From this discussion we infer that (4.12) is the appropriate stability criterion. Of course, this discussion has neglected all boundary effects; however, numerical experience has shown that if the right hand boundary is treated in an implicit manner as for example in Eqs. (4.5) and (4.6), then stability is determined by the treatment at the interior points.

## 5. GALERKIN METHOD WITH B-SPLINES

When the literature on computational methods in compressible hydrodynamics is examined, the overwhelming tendency is to use the method of characteristics or finite difference methods. However, finite difference methods involve some difficulties in the satisfaction of boundary conditions. The finite element method using a Galerkin procedure largely avoids these difficulties, and therefore offer a potentially very attractive alternative. Finite element methods have been used in a wide variety of flow problems (cf. ref. [9]), but to the best of our knowledge, these methods have not been implemented for the solution of waterhammer transients. In the present application, we have used a Galerkin procedure with an approximating subspace generated by a B-spline basis in order to reduce the system of partial differential equations to a system of ordinary differential equations [10]. The system of ODE's is then solved by using an ODE solver based on the GEAR code [11].

### Method of Lines

In the method of lines, one reduces the system of partial differential equations to a system of ordinary differential equations. Let $\theta(x,t) = (H(x,t),u(x,t))$, and assume that at each fixed time t, $\theta(x,t)$ can be approximated by piecewise polynomials in x generated by B-spline basis sets. Specifically, let the interval [0,L] be subdivided by a set of points, called breakpoints, as $\pi$: $0 = \eta_1 < \eta_2 < \ldots < \eta_\ell < \eta_{\ell+1} = L$.

Relative to this partition $\pi$, let $P_{k,\pi,\nu}$ denote the space of piecewise polynomials $F = \{f_i : 1 \le i \le \ell\}$ of order k (degree = k-1) and smoothness $\bar{\nu} = \{\nu_j\}_{j=2}^{\ell}$ (i.e. continuity of derivatives of F up to order $\nu_i$-1 at $\eta_i$) at the interior breakpoints. Then

$$\dim P_{k,\pi,\nu} = n = k\ell - \sum_{i=2}^{\ell} \nu_i \ , \tag{5.1}$$

where the first term represents the total number of coefficients of $\ell$ polynomial pieces and the second term is the total number of smoothness constraints

imposed at the interior breakpoints. We then seek an approximate solution of the form

$$\theta(x,t) = \sum_{i=1}^{n} \Omega_i(t) w_i(x) \ , \tag{5.2}$$

where $\Omega_i(t) = (H_i(t), u_i(t))'$ are unknown time dependent coefficients, and $\{w_i(x): \ 1 \le i \le n\}$ is a B-spline basis for the space $P_{k,\pi,\nu}$. The governing equations for the coefficients $\{\Omega_i(t): \ 1 \le i \le n\}$ are determined via a Galerkin procedure. However, before discussing this aspect, we will review some important features of B-splines.

B-Splines Basis

An excellent discussion of B-splines and an algorithm for generating these splines is given in refs. [12,13]. Tc generate a B-spline basis for the space $P_{k,\pi,\nu}$, define

$$g_k(s;\eta)_+^{k-1} = \begin{cases} (s-\eta)^{k-1} & s \ge \eta \\ 0 & s < \eta \end{cases} \ , \tag{5.3}$$

and let the set of multiple knots $\{\xi_i\}_{i=1}^{n+k}$ be defined by

$$\xi_1 = \ldots = \xi_k = \eta_1 \ ,$$

$$\xi_{k+1} = \ldots = \xi_{k+d} = \eta_2 \ ,$$

$$\vdots$$

$$\xi_{k+d_2+\ldots+d_{j-1}+1} = \ldots = \xi_{k+d_2+\ldots+d_j} = \eta_j \ , \quad j \le \ell \ ,$$

$$\vdots$$

$$\xi_{n+1} = \ldots = \xi_{n+k} = \eta_{\ell+1} \ .$$

The first and last breakpoints $\eta_1$ and $\eta_{\ell+1}$ have multiplicity k and the interior breakpoints have multiplicity $d_j = k-\nu_j$. The above construction of knots is shown schematically in Fig. 5.1. With each knot, we associate the B-spline $M_{i,k}(\eta)$ defined as the $k^{th}$ divided difference (see, for example, Steffensen [14]) of $g_k(s;\eta)$ in s on the set of knots $\xi_i,\ldots,\xi_{i+k}$, i.e.

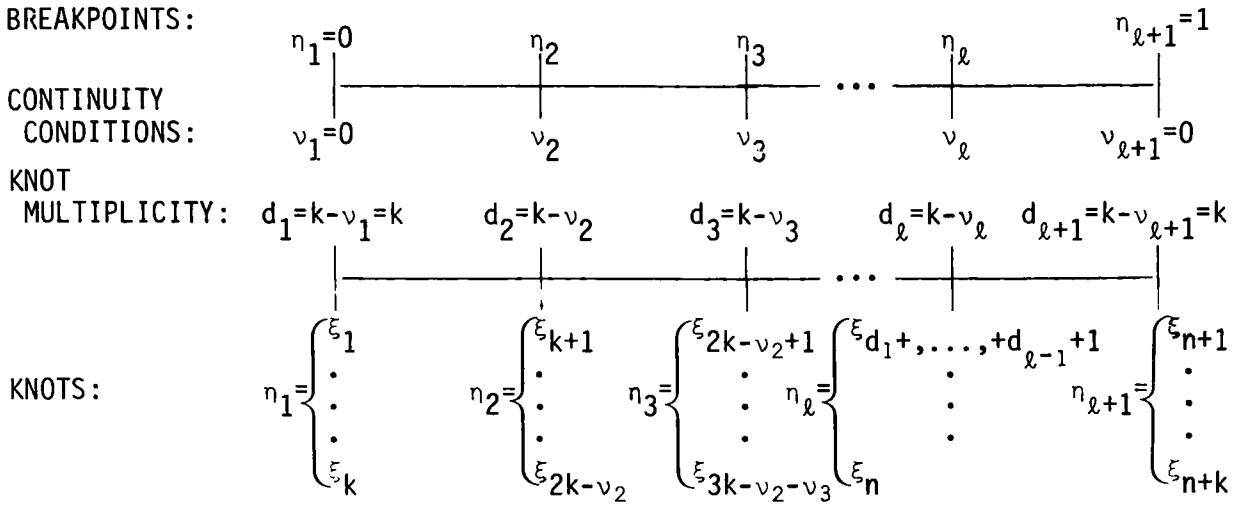


Fig. 5.1 Schematic diagram showing construction of knots

$$M_{i,k}(\eta) = g_k(\xi_i,\ldots,\xi_{i+k};\eta) = g_k(\xi_{i+1},\ldots,\xi_{i+k};\eta) - g_k(\xi_i,\ldots,\xi_{i+k-1};\eta)\,/(\xi_{i+k}-\xi_i)\ . \tag{5.4}$$

If the knots $\xi_i,\ldots,\xi_{i+k}$ are distinct, then

$$M_{i,k}(\eta) = g_k(\xi_i,\ldots,\xi_{i+k};\eta) = \sum_{j=0}^{k}\left\{g_k(\xi_{i+j};\eta)\left[\prod_{\substack{q=0\\ q\neq j}}^{k}(\xi_{i+j}-\xi_{i+q})\right]\right\}\ , \tag{5.5}$$

from which it follows that $M_{i,k}(\eta)$ is a linear combination of $(\xi_{i+j}-\eta)_+^{k-1}$. Thus, from Eqs. (5.3) and (5.5), we have

$$M_{i,k}(\eta) = 0 \quad \text{for} \quad \eta \notin [\xi_i,\xi_{i+k}]\ , \tag{5.6}$$

which implies that $M_{i,k}(\eta)$ has its support in $[\xi_i,\xi_{i+k}]$. If, however, $\xi_i,\ldots,\xi_{i+k}$ are not all distinct, then the divided difference given by Eq. (5.5) will also contain derivatives of $(\xi_{i+j}-\eta)_+^{k-1}$ with respect to coincident knots. Precisely, if $\zeta_1,\ldots,\zeta_L$ (where $\zeta_j$ is equal to some breakpoint in the set $\pi$) are the distinct points among $\xi_i,\ldots,\xi_{i+k}$ and if each $\zeta_j$ appears $d_j \le k$ times among them, $j=1,\ldots,L$, then $M_{i,k}$ is a linear combination of the functions

$$(\zeta_j-\eta)_+^{k-q} \quad 1 \le q \le d_j = k-\nu_j, \qquad j=1,\ldots,L\ .$$

Thus, $M_{i,k}(\eta)$ has the following properties: (i) it is a piecewise polynomial of order k having breakpoints only at $\zeta_j,\ldots,\zeta_L$; (ii) since $(\zeta_j-\eta)_+^{k-d_j}$ has $k-d_j-1$ continuous derivatives at $\eta = \xi_j$, it follows that

$$D^{(\mu)}M_{i,k}(\zeta_j^-) = D^{(\mu)}M_{i,k}(\zeta_j^+) \quad \text{for} \quad 0 \le \mu \le k-1-d_j, \quad j=1,\ldots,L \ ,$$

where $D^{(\mu)}$ denotes the derivative of order $\mu$; and (iii) for $\eta > \xi_{i+k}$ it follows from Eq. (5.3) that $M_{i,k}(\eta) = 0$ and for $\eta < \xi_i$, $M_{i,k}(\eta)$ is the $k^{th}$ divided difference of a polynomial of degree k-1; hence, $M_{i,k}(\eta) = 0$. Thus, $M_{i,k}(\eta)$ has its support in $(\xi_i,\xi_{i+k})$.

The basis that will be used for the approximating subspace are the normalized B-splines defined by

$$\begin{aligned} N_{i,k}(\eta) = (\xi_{i+k}-\xi_i)M_{i,k}(\eta) &= g_k(\xi_{i+1},\ldots,\xi_{i+k};\eta) \\ &\quad - g_k(\xi_i,\ldots,\xi_{i+k-1};\eta) \ , \end{aligned} \tag{5.7}$$

where $N_{i,k}(\eta)$ has the following properties:

(i) normalization property:

$$\sum_{i=1}^{n} N_{i,k}(\eta) \equiv 1 \ ; \tag{5.8}$$

(ii) convex recursion property:

$$\begin{aligned} N_{i,k}(\eta) = &\frac{\eta - \xi_i}{\xi_{i+k-1}-\xi_i} N_{i,k-1}(\eta) \\ &+ \frac{\xi_{i+k} - \eta}{\xi_{i+k}-\xi_{i+1}} N_{i+1,k-1}(\eta) \ , \quad \text{for} \quad \xi_i \le \eta < \xi_{i+k} \ , \end{aligned} \tag{5.9}$$

with $N_{i,1}(\eta)$ defined as

$$N_{i,1}(\eta) = \begin{cases} 1 & \xi_i \le \eta < \xi_{i+1} \\ 0 & \text{otherwise} \end{cases} \ . \tag{5.10}$$

Since $N_{i,1}(\eta) > 0$ for $\eta \in (\xi_i,\xi_{i+1})$ it follows from Eq. (5.9) that $N_{i,k}(\eta) > 0$ for $\eta \in (\xi_i,\xi_{i+k})$. The following explicit representation for $N_{1,k}(\eta)$ and $N_{n,k}(\eta)$ are given below for use in the application of boundary conditions:

$$N_{1,k}(\eta) = (\xi_{k+1}-\eta)^{k-1}/(\xi_{k+1}-\xi_1)^{k-1} , \quad \text{for } \xi_1 \le \eta \le \xi_{k+1} , \tag{5.11}$$

$$N_{n,k}(\eta) = (\eta-\xi_n)^{k-1}/(\xi_{n+k}-\xi_n)^{k-1} , \quad \text{for } \xi_n \le \eta \le \xi_{n+k} . \tag{5.12}$$

The application of Eq. (5.11) at $\eta = \eta_1 = \xi_1$ and of Eq. (5.12) at $\eta = \eta_{\ell+1} = \xi_{n+k}$ gives

$$N_{1,k}(\eta_1) = 1 , \qquad N'_{1,k}(\eta_1) = -(k-1)/(\eta_2-\eta_1) , \tag{5.13a}$$

$$N_{n,k}(\eta_{\ell+1}) = 1 , \qquad N'_{n,k}(\eta_{\ell+1}) = (k-1)/(\eta_{\ell+1}-\eta_\ell) . \tag{5.13b}$$

Since $N_{i,k}(\eta) \ge 0$ for $1 \le i \le n$ and $\eta \in [\eta_1\ \eta_{\ell+1}]$; therefore, from normalization property (5.8), it follows that

$$N_{i,k}(\eta_1) = 0, \text{ for } 1 < i \le n, \qquad N_{i,k}(\eta_{\ell+1}) = 0, \text{ for } 1 \le i < n . \tag{5.14a,b}$$

For the values of the derivatives of $N_{i,k}(\eta)$ at the end breakpoints, we start by considering the behavior of $N_{i,k}(\eta)$ at $\eta = \eta_1$ for $2 < i \le n$. Let us first consider the case $k+1 \le i \le n$ then since $N_{i,k}(\eta)$ has its support in $(\xi_i,\xi_{i+k})$ with $\xi_i \ge \eta_2$, it follows that $N_{i,k}(\eta) \equiv 0$ for $\eta < \eta_2$; thus $N_{i,k}(\eta)$ and all its derivatives will vanish at $\eta = \eta_1$. Next, we consider $2 < i \le k$, and in particular the case $i = 3$. Since $N_{3,k}(\eta)$ is a $k^{th}$ divided difference over the set $\xi_3,\ldots,\xi_{k+3}$ where $\xi_3 = \ldots = \xi_k(=\eta_1)$ appear $k-2$ times, this divided difference $N_{3,k}(\eta)$ has a knot of multiplicity $d = k-2$ at $\eta = \eta_1$. Since the smoothness index $\nu$ for $N_{3,k}(\eta)$ at $\eta_1$ satisifes the relation $\nu = k-d = k-(k-2) = 2$, we see that $N_{3,k}(\eta)$ has a continuous derivative at $\eta = \eta_1$. Now $N_{3,k}(\eta) \equiv 0$ for $\eta < \eta_1$; therefore $N'_{3,k}(\eta_1) = 0$. When $3 < i \le k$, a similar argument shows that $N_{i,k}(\eta)$ has $i-2$ continuous derivatives at $\eta = \eta_1$, thus $N'_{i,k}(\eta_1) = 0$ for $2 < i \le k$. More generally, we have

$$N^{(q)}_{i,k}(\eta_1) = 0, \quad \text{for } 0 \le q \le i-2 \text{ and } 2 \le i \le k . \tag{5.15}$$

Here we have used Eq. (5.14a) for the case $i = 2$. From the normalization property (5.8) we have

$$\sum_{i=1}^{n} N'_{i,k}(\eta) \equiv 0, \quad \text{for} \quad \eta \in [\eta_1, \eta_{\ell+1}] \ . \tag{5.16}$$

The use of Eq. (5.15) in Eq. (5.16) gives us

$$N'_{1,k}(\eta_1) + N'_{2,k}(\eta_1) = 0 \ , \tag{5.17}$$

with $N'_{1,k}(\eta_1)$ given by Eq. (5.13a). Analogous argument will show that

$$N^{(q)}_{i,k}(\eta_{\ell+1}) = 0, \quad \text{for} \quad 0 \le q \le n\text{-}i\text{-}1 \quad \text{and} \quad n\text{-}k\text{+}1 \le i \le n\text{-}1 \ . \tag{5.18}$$

Thus, from Eq. (5.16) and Eq. (5.18), we obtain

$$N'_{n-1,k}(\eta_{\ell+1}) + N'_{n,k}(\eta_{\ell+1}) = 0 \tag{5.19}$$

with $N'_{n,k}(\eta_{\ell+1})$ given by Eq. (5.13b).

For a graphic illustration of normalized B-splines, Fig. 5.2 gives the plot of $N_{i,k}(\eta)$ and Fig. 5.3 that of derivative of $N'_{i,k}(\eta)$ for $\ell$=3, k=4, $\nu$=2 and n=8 with $\eta$ partitioned as indicated in these figures.

Approximate Equations

In terms of normalized B-splines, expansion (5.2) takes the form

$$\theta(x,t) = \sum_{j=1}^{n} \Omega_j(t) N_{j,k}(x) \ , \tag{5.20}$$

where $\Omega_j(t) = (H_j(t), u_j(t))'$.

Of course, the basis functions $N_{j,k}(x)$ have local support; so that for a given x, the number of non-zero terms in expansion (5.20) is less than n. More specifically, each $N_{j,k}(x)$ is non-zero only in the interval $\{x: \ \xi_j \le x \le \xi_{j+k}\}$; hence when $x \in (\eta_s, \eta_{s+1})$, $N_{j,k}(x) \not\equiv 0$ for $\hat{J} = J\text{-}k\text{+}1 \le j \le J$ where $J = k + \sum_{r=2}^{s}(k\text{-}\nu_r)$ for $2 \le s \le \ell$. Thus expansion (5.20) becomes

$$\theta(x,t) = \sum_{j=\hat{J}}^{J} \Omega_j(t) N_{j,k}(x) \quad \text{for} \quad x \in (\eta_s, \eta_{s+1}), \quad 1 \le s \le \ell \ . \tag{5.21}$$

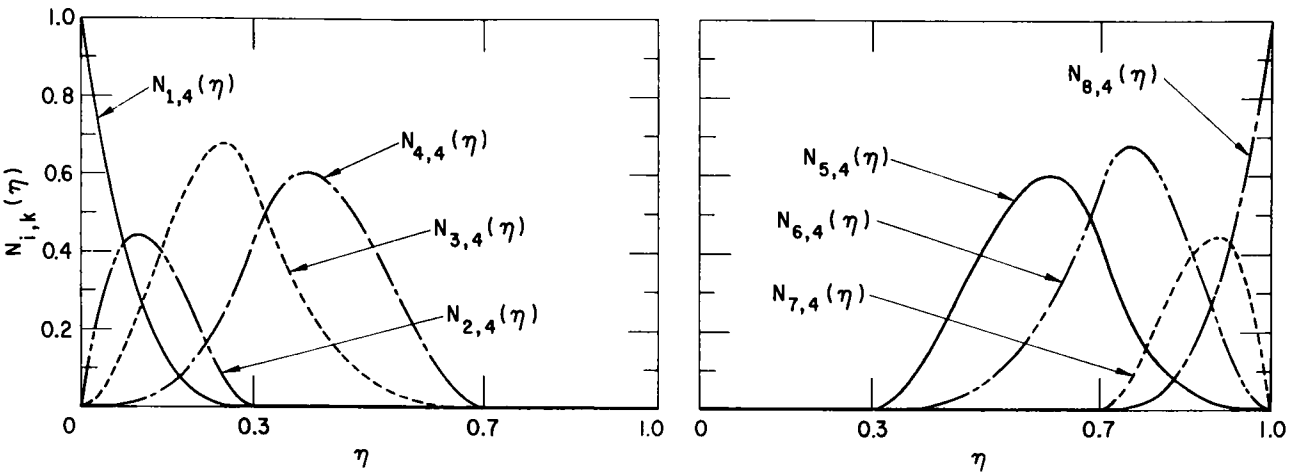


Fig. 5.2 Graphs of B-splines $N_{i,k}(\eta)$ for $k = 4$, $\nu = 2$ and $\ell = 3$ with breakpoints at $\eta_i = 0$, 0.3, 0.7 and 1.0

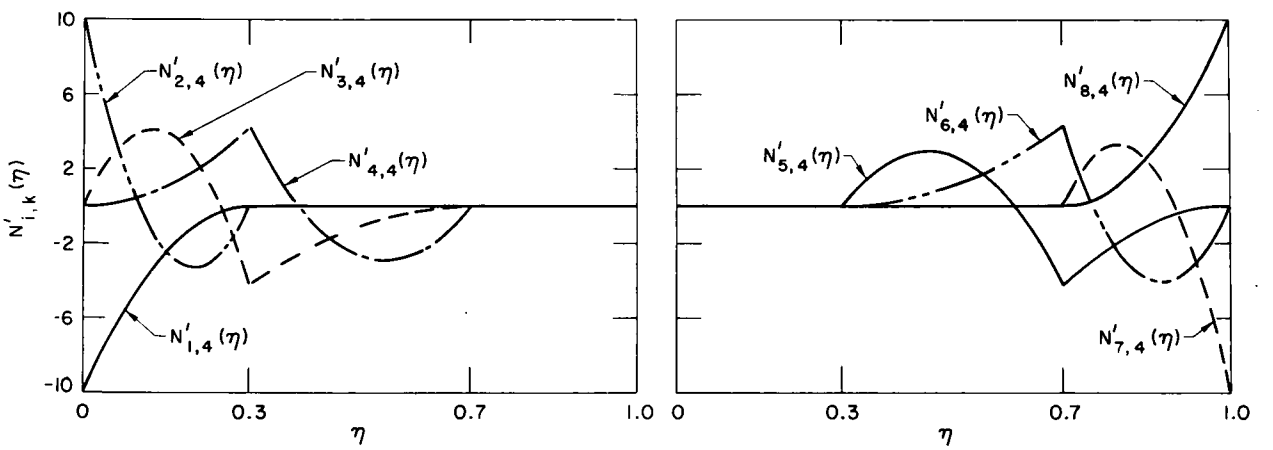


Fig. 5.3 Graphs of the first derivatives of B-splines $N_{i,k}(\eta)$ for $k = 4$, $\nu = 2$ and $\ell = 3$ with breakpoints at $\eta = 0$, 0.3, 0.7 and 1.0

Now, consider the Galerkin procedure for the system (2.7) and (2.10). Starting with the boundary condition (2.19) on the head, we find from conditions (5.13),(5.14) that

$$H_{0R} = H(0,t) = \sum_{j=1}^{n} H_j(t)N_{j,k}(0) = H_1(t) \ . \tag{5.22}$$

The right boundary condition takes the form

$$u_n(t) = \tau(t)u_0\sqrt{H_n(t)/H_0} \ . \tag{5.23}$$

These boundary conditions imply that the set $T_H = \{N_{j,k}: \ 2 \le j \le n\}$ can be used as test functions in Eq. (2.7), and the set $T_u = \{N_{j,k}: \ 1 \le j \le n-1\}$ can be used as test functions in Eq. (2.1). Using expansion (5.20) in Eqs. (2.7) and (2.10), with the test set $T_H$ on Eq. (2.7) and the test set $T_u$ on Eq. (2.10), we have the following system.

$$\sum_{j=1}^{n}\left\{\dot{H}_j(t)\langle N_{j,k},N_{i,k}\rangle + H_j(t)\langle uN'_{j,k},N_{i,k}\rangle + \frac{a^2}{g}u_j(t)\langle N'_{j,k},N_{i,k}\rangle\right\} = 0 \ , \tag{5.24}$$

$$\text{for } 2 \le i \le n \ .$$

$$\sum_{j=1}^{n}\left\{\dot{u}_j(t)\langle N_{j,k},N_{i,k}\rangle + u_j(t)\langle uN'_{j,k},N_{i,k}\rangle + gH_j(t)\langle N_{j,k},N_{i,k}\rangle + \frac{f}{2D}u_j(t)\langle |u|N_{j,k},N_{i,k}\rangle\right\} = 0 \ , \tag{5.25}$$

$$\text{for } 1 \le i \le n-1 \ ,$$

where $\dot{H}_j(t) = \frac{d}{dt}H_j(t)$, $\dot{u}_j(t) = \frac{d}{dt}u_j(t)$, and

$$\langle w,v\rangle = \int_0^L w(x)v(x)dx \ . \tag{5.26}$$

The local support of the basis functions is used in the evaluation of the integrals appearing in Eqs. (5.24) and (5.25). As an example, we consider

$$<uN'_{j,k},N_{i,k}> = \int_0^L u(x,t)N'_{j,k}(x)N_{i,k}(x)dx$$
$$= \sum_{s=1}^{\ell} \int_{\eta_s}^{\eta_{s+1}} u(x,t)N'_j(x)N_{i,k}(x)dx \ . \qquad (5.27)$$

Consider a fixed value for s, $1 \le s \le \ell$, then the integral over $[\eta_s,\eta_{s+1}]$ appearing in Eq. (5.27) will be non-zero for certain values of j and i. Specifically, set $J = J(s) = k + \sum_{r=2}^{s}(k-\nu_r)$ and $\hat{J} = \hat{J}(s) = J(s)-k+1$, then $N'_{j,k}(x)N_{i,k}(x) \not\equiv 0$ in $(\eta_s,\eta_{s+1})$ only when $\hat{J}(s) \le i,j \le J(s)$. Each integral is evaluated by Gauss-Legendre quadrature over $(\eta_s,\eta_{s+1})$ so that

$$\int_{\eta_s}^{\eta_{s+1}} u(x,t)N'_{j,k}(x)N_{i,k}(x)dx = \sum_{\mu=1}^{p} w_\mu u(x_\mu,t)N'_{j,k}(x_\mu)N_{i,k}(x_\mu) \qquad (5.28)$$

where $\{x_\mu,w_\mu\}$ are the Gaussian points and weights relative to the interval $(\eta_s,\eta_{s+1})$. The number of points p is restricted to $p \ge k-1$ with the choice $p = k-1$ providing a quadrature error which is not larger than the truncation error due to the choice of B-spline order and mesh (cf. Strang [15]).

The equations (5.22 - 5.25) form a system of mixed algebraic-differential equations of the following form:

$$\begin{aligned} &a) \quad 0 = g(y,z,t) \\ &b) \quad A\dot{z} = f(y,z,t) \end{aligned} \qquad (5.29)$$

where $y = (H_1(t),u_{n+1}(t))'$, $z = (H_2(t),\ldots,H_{n+1}(t),u_1(t),\ldots,u_n(t))'$ and A is a band matrix. This system is solved using a variant of the GEAR ODE solver [11].

Some observations of Galerkin type approximations are in order. First, we observe that any Galerkin type approximation to a transient problem leads to an implicit system in the sense that a coefficient matrix A is generated as in Eq. (5.29). This means that any time integration scheme, whether it be single step or multistep, will have to be an implicit scheme. Second, the use of B-splines of any order k and smoothness $\nu$, $0 \le \nu \le k-1$ provides a family of approximations. For example, the choice k=4 leads to the three approximations: smooth cubics ($\nu$=3), Hermite cubics ($\nu$=2), and continuous cubics ($\nu$=1).

## 6. COMPARISON OF LINEAR AND QUADRATIC INTERPOLATION FOR THE METHOD OF CHARACTERISTICS

From section 2, we recall that there are two approximations in the method of characteristics. First, there is the approximation (3.10) to the integral which generates an asymptotic error of order $O(\delta t^2)$. The second approximation involves the interpolation of the grid point values at a given time value. We have discussed the use of linear and quadratic interpolation in section 3. Here we will compare the errors encountered with these two schemes and we shall establish the benchmark values for the two cases of water hammer problems corresponding to choices m=1 and 2.

Before making the comparison, we know from experience for small density changes and at low velocities that at any given time, the pressure profile is almost linear along the pipe (i.e. nearly constant pressure gradient) and that the velocity profile at any time is smooth and has no steep gradients. Thus, we expect good accuracy with a very coarse spatial mesh.

In Tables 6.1 and 6.2, we present the data at three different points $(\bar{x},t)$. The first point (0.6,2.147) is at an intermediate point in the pipe and at a time t = 2.147. The second point (1.0,5.9) is at the valve end at the time t = 5.9 when the valve has closed. The third point (0.2,7.728) is at a point near the reservoir end at the time when the flow has reversed. The benchmark values are taken as the quadratic interpolation with n = 80.

In Table 6.1, we present the results for the case m = 1. We first observe that in all cases, the accuracy is very good even when N = 5 where the relative percentage error (% r.e.) does not exceed 2%. We also observe that the greatest errors occur as the severity of the transient increases as, for example, near t = 7.728 sec. for the case of m = 2 as compared to that of m = 1. For this reason we will use the time t = 7.728 when discussing other numerical methods.

Surprisingly, the convergence is not firmly established from these tables. For example, consider the velocities in Table 6.1c and four successive differences for N = 5,10,...,80. Then we find:

| | | | | |
|---|---|---|---|---|
| Linear | 4.176(-3) | 0.234(-3) | 0.447(-3) | 0.457(-3) |
| Quadratic | 2.488(-3) | 0.118(-3) | 0.252(-3) | 0.248(-3) |

TABLE 6.1a Pressure Head and Velocity at $(\bar{x},t)$

N = # variables, $\bar{x} = x/L = 0.6$, $t = 2.147$ sec, $u_0 = 3.5$ ft/sec, $\tau = (1-t/tc)^{m}$ (m=1)

| | | N = 5 | N = 10 | N = 20 | N = 40 | N = 80 |
|---|---|---|---|---|---|---|
| Linear Interpolation | H | 368.3323 | 368.3823 | 368.4074 | 368.4200 | 368.4262 |
| | % r.e. | 2.55(-2) | 1.20(-2) | 0.52(-2) | 0.17(-2) | |
| | u | 2.6635 | 2.6638 | 2.6639 | 2.6640 | 2.6640 |
| | % r.e. | 1.88(-2) | 0.751(-2) | 0.375(-2) | -- | |
| Quadratic Interpolation | H | 368.3343 | 368.3832 | 368.4078 | 368.4202 | 368.4264 |
| | % r.e. | 2.50(-2) | 1.17(-2) | 0.51(-2) | 0.17(-2) | |
| | u | 2.6636 | 2.6638 | 2.6639 | 2.6640 | 2.6640 |
| | % r.e. | 1.50(-2) | 0.751(-2) | 0.375(-2) | -- | |

TABLE 6.1b Exit Pressure Head at Time of Valve Closure

N = # variables, $\bar{x} = x/L = 1.0$, $t = 5.9$ sec, $u_0 = 3.5$ ft/sec, $\tau = (1-t/tc)^{m}$ (m=1)

| | | N = 5 | N = 10 | N = 20 | N = 40 | N = 80 |
|---|---|---|---|---|---|---|
| Linear Interpolation | H | 391.9191 | 391.7973 | 391.7871 | 391.7816 | 391.7789 |
| | % r.e. | 36.0(-3) | 4.9(-3) | 0.23(-3) | 0.092(-3) | 0.0 |
| Quadratic Interpolation | H | 391.7937 | 391.7899 | 391.7834 | 391.7798 | 391.7780 |
| | % r.e. | 4.01(-3) | 3.04(-3) | 0.14(-3) | 0.046(-3) | 0.0 |

TALBE 6.1c Pressure Head and Velocity at $(\bar{x},t)$

N = # variables, $\bar{x} = x/L = 0.2$, $t = 7.728$ sec, $u_0 = 3.5$ ft/sec, $\tau = (1-t/tc)^{m}$ (m=1)

| | | N = 5 | N = 10 | N = 20 | N = 40 | N = 80 |
|---|---|---|---|---|---|---|
| Linear Interpolation | H | 288.3149 | 287.8654 | 287.8335 | 287.7770 | 287.7197 |
| | % r.e. | 21.7(-2) | 6.1(-2) | 5.0(-2) | 3.1(-2) | |
| | u | -0.284862 | -0.289038 | -0.289272 | -0.289719 | -0.290176 |
| | % r.e. | 1.92 | 0.48 | 0.40 | 0.24 | |
| Quadratic Interpolation | H | 288.1615 | 287.7825 | 287.7586 | 287.7225 | 287.6894 |
| | % r.e. | 18.4(-2) | 3.2(-2) | 2.4(-2) | 1.2(-2) | |
| | u | -0.287322 | -0.289810 | -0.289928 | -0.290180 | -0.290428 |
| | % r.e. | 1.1 | 0.21 | 0.17 | 0.085 | |

For convergence we would expect these differences to be decreasing. This is not happening yet in the linear case, but may be starting in the quadratic case. In any case, if we do have convergence it is clear that we are not in the asymptotic range where a rate of convergence can be determined.

In later sections we will be comparing various approximate solutions; hence it is desirable to establish benchmark values. As the benchmark values, we intend to use the method of characteristics with N = 80 and quadratic interpolation. In an attempt to estimate the number of significant digits that we are justified in using for these benchmark values, we will consider the effect of linear extrapolation on the pressure and velocity. For example, consider Table 6.1c, and extrapolate linearly these values, then we obtain the following table.

TABLE 6.1d Linear Extrapolation of Pressure Head and Velocity

| N | H | H (extrapolated) | u | u (extrapolated) |
|---|---|---|---|---|
| 5 | 288.1615 | | -0.287322 | |
| 10 | 287.7825 | 287.4035 | -0.289810 | -0.292298 |
| 20 | 287.7586 | 287.7735 | -0.289928 | -0.290046 |
| 40 | 287.7225 | 287.6864 | -0.290180 | -0.290432 |

The extrapolated pressure 287.6864 can be compared with the benchmark pressure of 287.6894 (see Table 6.1c) from which we infer that we can have some confidence in four significant digits for the benchmark pressure. When we compare the extrapolated velocity -0.290432 with the benchmark value -0.290428, we infer that we can have confidence in three significant digits for the benchmark velocity.

In Table 6.2 we present the case of m = 2. Here, as we can see, the errors are somewhat greater than those for the case m = 1. Qualitatively, the comparison between linear and quadratic interpolation, as well as the behavior of the error with N, is the same as in the case m = 1.

TABLE 6.2a Pressure Head and Velocity at $(\bar{x},t)$

N = # variables, $\bar{x} = x/L = 0.6$, $t = 2.147$ sec, $u_0 = 3.5$ ft/sec, $\tau = (1-t/tc)^2$ (m=2)

| | | N = 5 | N = 10 | N = 20 | N = 40 | N = 80 |
|---|---|---|---|---|---|---|
| Linear Interpolation | H | 427.1372 | 427.2366 | 427.2858 | 427.3103 | 427.3225 |
| | % r.e. | 4.07(-2) | 1.74(-2) | 0.590(-2) | 0.295(-2) | |
| | u | 1.8880 | 1.8883 | 1.8885 | 1.8886 | 1.8886 |
| | % r.e. | 3.18(-2) | 1.59(-2) | 0.530(-2) | -- | |
| Quadratic Interpolation | H | 427.1433 | 427.2393 | 427.2872 | 427.3110 | 427.3229 |
| | % r.e. | 3.93(-2) | 1.68(-2) | 0.557(-2) | 0.279(-2) | |
| | u | 1.8881 | 1.8884 | 1.8885 | 1.8886 | 1.8886 |
| | % r.e. | 2.65(-2) | 1.06(-2) | 0.530(-2) | -- | |

TABLE 6.2b Exit Pressure Head at Time of Valve Closure

N = # variables, $\bar{x} = x/L = 1.0$, $t = 5.9$ sec, $u_0 = 3.5$ ft/sec, $\tau = (1-t/tc)^2$ (m=2)

| | | N = 5 | N = 10 | N = 20 | N = 40 | N = 80 |
|---|---|---|---|---|---|---|
| Linear Interpolation | H | 301.3029 | 300.7782 | 300.7585 | 300.7489 | 300.7441 |
| | % r.e. | 18.6(-2) | 1.16(-2) | 0.509(-2) | 0.246(-2) | |
| Quadratic Interpolation | H | 300.7768 | 300.7538 | 300.7466 | 300.7432 | 300.7415 |
| | % r.e. | 1.12(-2) | 0.353(-2) | 0.113(-2) | 0.057 | |

TABLE 6.2c Pressure Head and Velocity at $(\bar{x},t)$

N = # variables, $\bar{x} = x/L = 0.2$, $t = 7.728$ sec, $u_0 = 3.5$ ft/sec, $\tau = (1-t/tc)^2$ (m=2)

| | | N = 5 | N = 10 | N = 20 | N = 40 | N = 80 |
|---|---|---|---|---|---|---|
| Linear Interpolation | H | 308.0662 | 306.3922 | 306.2763 | 306.0665 | 305.8535 |
| | % r.e. | 0.720 | 0.173 | 0.135 | 0.106 | |
| | u | -0.294277 | -0.312257 | -0.313821 | -0.315837 | -0.317713 |
| | % r.e. | 7.34 | 1.68 | 1.19 | 0.552 | |
| Quadratic Interpolation | H | 307.4694 | 306.0826 | 305.9967 | 305.8642 | 305.7419 |
| | % r.e. | 0.525 | 0.0714 | 0.0433 | 0.040 | |
| | u | -0.304867 | -0.315368 | -0.316374 | -0.317590 | -0.318653 |
| | % r.e. | 4.01 | 0.700 | 0.383 | 0.334 | |

# 7. COMPARISON OF GALERKIN, LAX, AND METHOD OF CHARACTERISTICS

## Comparison of Several Galerkin Approximations

We begin this section by comparing various Galerkin approximations to the water hammer problem. Recall from section 5 that k denotes the order (degree = k-1) of the piecewise polynomials used in the Galerkin approximation. Furthermore, for any k, we can choose any value of $\nu$, $0 \le \nu \le k-1$ where $\nu$ is the smoothness of the piecewise polynomials. That is, if f(x) is a piecewise polynomial with smoothness index $\nu$, then $f^{(\nu-1)}(x)$ is continuous. If the length L of the pipe is divided into $\ell$ subintervals, then we see that we have the three parameters $(k,\nu,\ell)$ at our disposal when generating Galerkin approximations to the water hammer problem. For a given set $(k,\nu,\ell)$, the number of variables (for either the velocity u or the pressure head H) will be

$$N = k + (k-\nu)(\ell-1) \ . \tag{7.1}$$

With the three parameters at our disposal we can generate a variety of approximations to the water hammer problem. We will start the numerical study by comparing the following six Galerkin approximations.

$k = 4, \nu = 3$ ... Piecewise cubic polynomials with continuous second derivatives. These are the smooth cubic splines.

$k = 4, \nu = 2$ ... Piecewise cubic polynomials with continuous first derivatives. These are the Hermite cubic splines.

$k = 4, \nu = 1$ ... Piecewise cubic polynomials which are continuous.

$k = 3, \nu = 2$ ... Piecewise quadratic polynomials with continuous first derivatives (smooth quadratics).

$k = 3, \nu = 1$ ... Piecewise quadratic polynomials which are continuous.

$k = 2, \nu = 1$ ... Piecewise linear polynomials which are continuous.

Since we are using an ODE solver [11] to solve the system of ordinary differential equations, the accuracy of the time integration is independent of the accuracy of the spatial approximation. Hence we wish to fix the accuracy of the time integration for all six approximations. Table 7.1 illustrates, for our particular approximation, the effect of varying the tolerance in the local time truncation error parameter. In this table we compare the pressure and

TABLE 7.1 Effect of Time Integration Tolerance in ODE for Galerkin Approximation with k = 3, $\nu = 1$, $\ell = 2$, t = 7.728

| | EPS = $10^{-6}$ | EPS = $16^{-9}$ | EPS = $10^{-6}$ | EPS = $10^{-9}$ |
|---|---|---|---|---|
| $\bar{x}$ = .2 | 289.4342 | 289.4387 | -0.270184 | -0.270207 |
| .4 | 272.0870 | 272.0871 | -0.267719 | -0.267764 |
| .6 | 256.0881 | 256.0824 | -0.258748 | -0.258733 |
| .8 | 248.5941 | 248.5933 | -0.159387 | -0.159363 |

velocity at four locations in the pipe with a tolerance, EPS = $10^{-6}$ and EPS = $10^{-9}$ in the ODE solver. From this table we infer that the error due to the time tolerance EPS = $10^{-6}$ is beyond the fourth significant digit in both the pressure and the velocity. In comparing the six Galerkin approximations we have used EPS = $10^{-6}$ under the assumption that the error due to time integration is beyond the fourth significant digit for both the pressure and the velocity. At the end of section 6, we inferred that our benchmark values have at least four significant digits for the pressure and at least three significant digits for the velocity. Thus we feel justified in using EPS = $10^{-6}$ in the Galerkin approximations.

For the comparison of the six Galerkin approximations, we proceed as follows. For each approximation (specified k and $\nu$), we set N in Eq. (7.1) to two values 5 and 10 and determine $\ell$ so that this equation is satisfied. (There are some values of k and $\nu$ for which $\ell$ does not have an integer solution. In this case N = 4 and 9 are used.) Recall that N is the number of variables associated with either H or u; so that the dimension of the problem is 2N. For each triple $(k,\nu,\ell)$, we select the fixed time t = 7.728 where we measure the errors. For either the pressure or the velocity, let $y(\bar{x}_i)$ denote the benchmark values given in section 6 at the four interior points $\bar{x}_i = x_i/L$ = 0.2,0.4,0.6,0.8 along the pipe. If $\hat{y}(\bar{x}_i)$ denotes an approximation at these same points, we compute the following quantities.

a) $\varepsilon_i = \left[|y(\bar{x}_i) - \hat{y}(\bar{x}_i)|/|y(\bar{x}_i)|\right] \times 100$ (% relative error) ,

b) $\varepsilon_{max} = \max\{\varepsilon_i : 1 \le i \le 4\}$ ,

c) $\varepsilon_{mean} = \frac{1}{4} \sum_{i=1}^{4} \varepsilon_i$ ,

d) $\varepsilon_{r.m.s.} = \left[\frac{1}{4} \sum_{i=1}^{4} \varepsilon_i^2\right]^{\frac{1}{2}}$ .

For the pressure and the velocity, these quantities are given in the following two tables.

TABLE 7.2a Errors in the Pressure at t = 7.728

| | | $\varepsilon_{max}$ | | $\varepsilon_{mean}$ | | $\varepsilon_{r.m.s.}$ | |
|---|---|---|---|---|---|---|---|
| | | N = 5 | N = 10 | N = 5 | N = 10 | N = 5 | N = 10 |
| Cubic K = 4 | ν = 3 | 0.76 | 0.41 | 0.44 | 0.22 | 0.50 | 0.26 |
| | ν = 2 | 0.94* | 0.27 | 0.31 | 0.18 | 0.62 | 0.19 |
| | ν = 1 | 0.94* | 0.42 | 0.38 | 0.29 | 0.53 | 0.43 |
| Quadratic K = 3 | ν = 2 | 0.52 | 0.26 | 0.23 | 0.18 | 0.30 | 0.19 |
| | ν = 1 | 0.60 | 0.49 | 0.25 | 0.183 | 0.33 | 0.21* |
| Linear K = 2 | ν = 1 | 0.47 | 0.33 | 0.20 | 0.18 | 0.26 | 0.23 |

TABLE 7.2b Errors in the Velocity at t = 7.728

| | | $\varepsilon_{max}$ | | $\varepsilon_{mean}$ | | $\varepsilon_{r.m.s.}$ | |
|---|---|---|---|---|---|---|---|
| | | N = 5 | N = 10 | N = 5 | N = 10 | N = 5 | N = 10 |
| Cubic K = 4 | ν = 3 | 9.6 | 4.7 | 4.4 | 3.1 | 5.5 | 3.3 |
| | ν = 2 | 12.8* | 6.9 | 6.6* | 2.2 | 8.4* | 3.5 |
| | ν = 1 | 12.8* | 8.0 | 6.6* | 2.9 | 8.4* | 4.2 |
| Quadratic K = 3 | ν = 2 | 14.3 | 3.7 | 6.8 | 2.6 | 8.6 | 2.8 |
| | ν = 1 | 6.9 | 2.6* | 3.1 | 1.1* | 4.0 | 1.4* |
| Linear K = 2 | ν = 1 | 10.5 | 5.4 | 6.6 | 3.0 | 7.5 | 3.7 |

The * indicates that N = 4 or 9 was used for that calculation.

Based on the data in this table, we draw the following conclusions.

- As far as the pressure is concerned, no one particular approximation stands out from the rest.
- As far as the velocity is concerned, the continuous quadratic ($k = 3$, $\nu = 1$) stands out from the rest. Moreover, the difference is significant; the error is generally less than half that for any of the other approximations.
- The use of high order approximations such as cubics appears to offer no advantage for problems of this type

From the results in Table 7.2, we select two Galerkin approximations for comparison with the Method of Characteristics and the Lax Method. The continuous quadratic ($k = 3$, $\nu = 1$) was selected since it has a significantly smaller error for a given number of variables than any other Galerkin approximation. The continuous linear ($k = 2$, $\nu = 1$) was selected because it has the same asymptotic error in the spatial approximation as the method of characteristics with linear interpolation and the Lax Method.

We next consider the rate of convergence of these two Galerkin approximations as the spatial mesh is refined. Using $\varepsilon_{max}$ and $\varepsilon_{mean}$ as defined in (7.2), Table 7.3 shows the per cent relative errors in the velocity at $t = 7.728$.

TABLE 7.3 Errors in the Velocity at $t = 7.728$

| | $\varepsilon_{max}$ | | | | $\varepsilon_{mean}$ | | | |
|---|---|---|---|---|---|---|---|---|
| | N = 5 | N = 10 | N = 20 | N = 37 | N = 5 | N = 10 | N = 20 | N = 37 |
| Quadratic ($k=3,\nu=1$) | 6.9 | 2.6* | 1.06* | 0.57 | 3.1 | 1.1* | 0.58* | 0.27 |
| Linear ($k=2,\nu=1$) | 10.5 | 5.4 | 1.86 | | 6.6 | 3.0 | 0.99 | |

From Table 7.3 we draw the following conclusions.

- Both approximations appear to be converging.
- Asymptotic rates of convergence are not established. Estimating rates, we find:

| | | | |
|---|---|---|---|
| $k = 3, \nu = 1$ | 1.5 | 0.92 | 1.1 |
| $k = 2, \nu = 1$ | 1.1 | 1.6 | |

  At best it would appear that the asymptotic rate may be about one for either of these approximations.

- Error for the quadratic ($K = 3, \nu = 1$) is about half the error for the linear approximation.

Comparison with Method of Characteristics and Lax Method

We now compare the method of characteristics, Galerkin, and the Lax method. For the method of characteristics we will use both the linear and the quadratic interpolation, while for the Galerkin methods we will use both the quadratic ($k = 3, \nu = 1$) and the linear ($k = 2, \nu = 1$). Thus our comparison will involve five approximations. The comparison will be on the basis of the error in the velocity at $t = 7.728$ and at the four interior points $\bar{x} = 0.2, 0.4, 0.6$, and 0.8. In addition, we shall also make a separate comparison at the reservoir end of the pipe $\bar{x} = 0.0$ which is, of course, a boundary point.

In Table 7.4 we compare the errors at the interior points for $N = 5$, 10, and 20. For the Lax method, in the column labeled $N = 20$, we have also given the error for $N = 40$.

TABLE 7.4 Errors in the Velocity at t = 7.728 at Some Interior Points, m = 1

| | | $\epsilon_{max}$ | | | $\epsilon_{mean}$ | | |
|---|---|---|---|---|---|---|---|
| | | N = 5 | N = 10 | N = 20 | N = 5 | N = 10 | N = 20 |
| Method of Char. | Linear | 2.9 | 0.39 | 0.31 | 1.6 | 0.17 | 0.098 |
| | Quadratic | 1.4 | 2.1 | 0.18 | 0.67 | 0.55 | 0.073 |
| Galerkin | Linear (K=2,ν=1) | 10.5 | 5.4 | 1.9 | 6.6 | 3.0 | 1.0 |
| | Quadratic (K=3,ν=1) | 6.9 | 2.6 | 1.1 | 3.1 | 1.1 | 0.6 |
| Lax | | 36.8 | 14.9 | 4.9 / 1.0 | 20.1 | 8.0 | 2.0 / 0.38 |

TABLE 7.5 Errors in Velocity at Reservoir at t = 7.728, m = 1

| | | N = 5 | % r.e. | N = 10 | % r.e. | N = 20 | % r.e. |
|---|---|---|---|---|---|---|---|
| Method of Char. | Linear | -0.290528 | 0.37 | -0.291675 | 0.03 | -0.291629 | 0.004 |
| | Quadratic | -0.297282 | 1.95 | -0.291940 | 0.12 | -0.291654 | 0.02 |
| Galerkin | Linear (K=2,ν=1) | -0.222270 | 23.8 | -0.288953 | 0.91 | -0.295564 | 1.36 |
| | Quadratic(K=3,ν=1) | -0.324467 | 11.3 | -0.290314 | 0.44 | -0.289659 | 0.66 |
| Lax | | -0.439976 | 50.9 | -0.258461 | 11.4 | -0.300397 | 3.0 |
| Benchmark value -0.291594 (MOD, Quad, N=80) | | | | Lax, N = 40 | | -0.291228 | 0.13 |

Before interpreting the data in Tables 7.4 and 7.5, we will present the same type of data for the case m = 2. We may note that in this case the transient responses are more severe than in the case m = 1. In particular, there are two flow reversals in the course of the transient. The first reversal occurs at approximately t = 3.864 sec. and the second at the usual time t = 5.9 sec. In Fig. 7.1 we illustrate the first flow reversal with a plot of velocities as a function of position at time t = 3.864 sec. for the cases m = 1 and 2. In addition, Fig. 7.2 shows the plots of pressure heads at x/L = 1 as a function of time for the cases of m = ½, 1, and 2. This figure clearly shows that pressure rise corresponding to m = 2 is much faster than the pressure rise corresponding to m = 1.

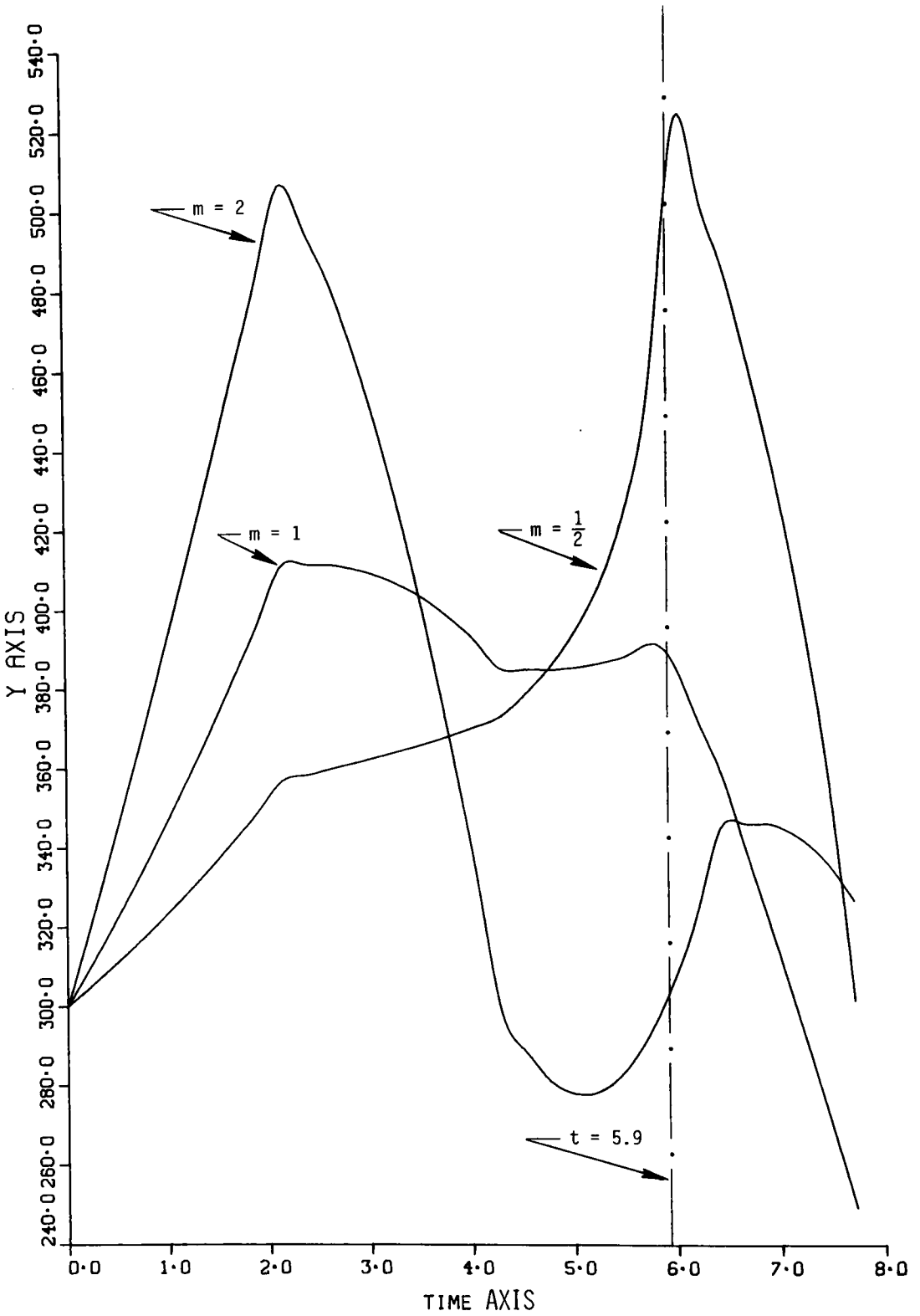


Fig. 7.1 Graphs of velocities at time t = 3.864 sec. for the cases m = 1 and 2

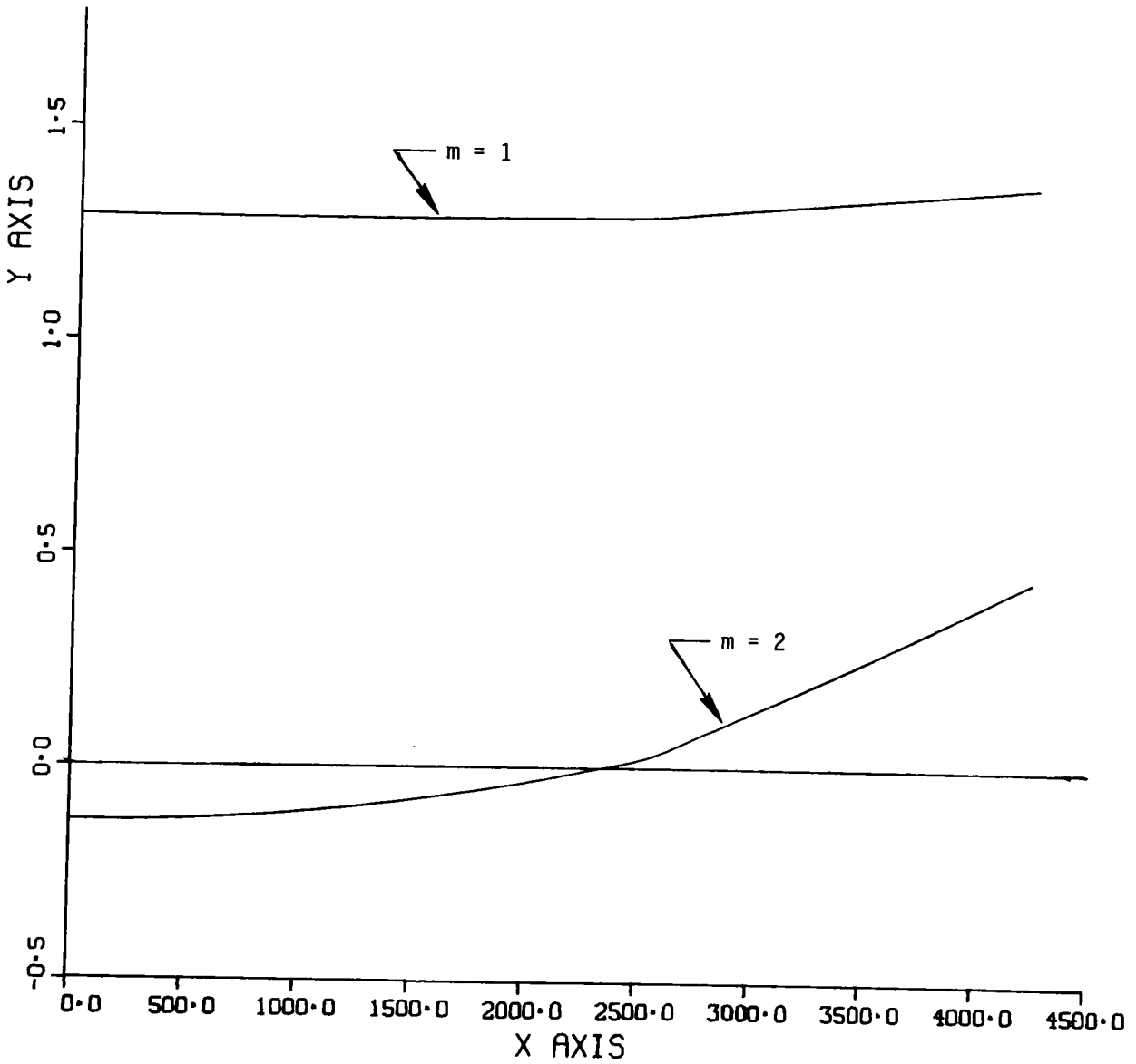


Fig. 7.2 Graphs of exit pressures as functions of time for the cases m = ½, 1, and 2

TABLE 7.6 Errors in Velocity at t = 7.728 at Some Interior Points, m = 2

| | | $\varepsilon_{max}$ | | | $\varepsilon_{mean}$ | | |
|---|---|---|---|---|---|---|---|
| | | N = 5 | N = 10 | N = 20 | N = 5 | N = 10 | N = 20 |
| Method of Char. | Linear | 7.7 | 2.0 | 1.5 | 2.3 | 0.57 | 0.41 |
| | Quadratic | 4.3 | 1.0 | 0.72 | 1.4 | 0.36 | 0.23 |
| Galerkin | Linear (K=2,ν=1) | 16.0 | 6.0 | 1.9 | 6.0 | 3.7 | 0.67 |
| | Quadratic(K=3,ν=1) | 7.6 | 2.9 | 1.4 | 3.2 | 2.3 | 0.72 |
| Lax | | 36.3 | 17.7 | 8.0<br>3.7 | 27.3 | 11.2 | 3.0<br>1.1 |

TABLE 7.7 Errors in Velocity at Reservoir at t = 7.728, m = 2

| | | N = 5 | % r.e. | N = 10 | % r.e. | N = 20 | % r.e. |
|---|---|---|---|---|---|---|---|
| Method of Char. | Linear | -0.317310 | 2.3 | -0.323787 | 0.29 | -0.324317 | 0.12 |
| | Quadratic | -0.343850 | 5.9 | -0.324916 | 0.06 | -0.324503 | 0.07 |
| Galerkin | Linear (K=2,ν=1) | -0.324023 | 0.22 | -0.331992 | 2.2 | -0.320250 | 1.4 |
| | Quadratic(K=3,ν=1) | -0.341145 | 5.1 | -0.320029 | 1.5 | -0.326486 | 0.54 |
| Lax | | -0.231881 | 28.6 | -0.293800 | 9.5 | -0.322220 | 0.77 |
| Benchmark value -0.324721 (MOC, Quad, N = 80) | | | | | N = 40 | -0.323058 | 0.51 |

Comparing the case m = 1 with the case m = 2, we see that the qualitative behavior is generally the same. There are two major exceptions, both involving the method of characteristics with quadratic (MOCQ) interpolation. In Table 7.4 we observe that when N = 10 the MOCQ is significantly less accurate than the method of characteristics (MOC). Moreover, in Table 7.5 we see that the MOCQ is significantly less accurate than MOC for N = 5, 10, and 20. But this same pattern is not seen in Table 7.6, but it occurs again for N = 5 in Table 7.7. The data and program was checked and additional computer runs made but with the same results. We have no ready explanation for this anomalous behavior.

We interpret the data in these tables as follows.

- For a given value of N, the method of characteristics (linear or quadratic) is significantly more accurate than Galerkin procedures -- generally twice as accurate.

- For a given value of N, Galerkin procedures are significantly more accurate than the Lax method -- generally more than twice as accurate.

- For a given value of N, the Lax method was surprisingly inaccurate. For example when N = 5, its maximum relative error at interior points was at least 36.8% which is more than 26 times the relative error for MOCQ. Asymptotically, the Lax method, Galerkin linear, and MOC all have spatial approximations of the same order; but for moderate values of N, the actual errors differ significantly.

- The Galerkin methods were solved with an ODE solver; thus they represent an example of the use of high order implicit time integration in a hyperbolic system. From these tables, we feel that Galerkin techniques offer no substantial advantage over the Lax method. We base this judgement on the following considerations.

  a) As N increases, the "rate" of error reduction is not very different for Galerkin and Lax.

  b) We have not shown the times for these calculations for two reasons.

     (i) Precise times are not readily available; thus we could not accurately compare MOC, MOCQ, and Lax. They all take about the same time.

     (ii) The Galerkin method was done with a general purpose package; whereas the others were done with special purpose codes. Thus we did not know how to accurately access the overhead in the package.

  However, in an effort to substantiate our conclusion regarding the Galerkin technique, we present some

representative CPU times for these calculations. The times are in seconds on an IBM 370/195, and represent the entire job cost.

TABLE 7.8 CPU Times for Various Methods

| | N = 5 | N = 10 | N = 20 | N = 40 | N = 80 |
|---|---|---|---|---|---|
| MOC | 1 | 1 | 2 | 4 | 14 |
| MOCQ | 1 | 1 | 2 | 7 | 26 |
| Gal. Lin. | 8 | 13 | 45 | | |
| Gal. Quad | 9 | 18 | 51 | | |
| Lax | 1 | 1 | 2 | 5 | |

Even with a substantial allowance for overhead, the Galerkin procedures do not appear competitive with even the Lax method for hyperbolic problems of this type.

- The method of characteristics, either linear or quadratic, is by far the best method for problems of this type. This conclusion takes into account the simplicity of the method, accuracy, and computational cost.

## 8. THE CASE OF A RIGID WALL

Certain specific methods such as Lax-Wendroff scheme [7,8] and the donor cell type difference method [15,16] require that the system of governing equations be in a conservative form. Since the case of an elastic wall does not lead to a conservative form of governing equations, we are obliged to study the case of a rigid wall which as demonstrated previously leads to a conservative form of the system of Eqs. (2.14) and (2.15) (with boundary conditions given by Eqs. (2.17), (2.18), (2.19b) and initial conditions given by Eqs. (2.20b) and (2.20c)).

It is worth noting that the system (2.7) and (2.10) is not equivalent to the system (2.14) and (2.15). To bring out the differences we proceed as follows. From Eq. (2.13c), we have

$$\rho = \rho_R g(H+C_R)/a^2;$$

thus

$$\frac{\partial \rho}{\partial t} = \frac{\rho_R g}{a^2}\frac{\partial H}{\partial t}, \quad \text{and} \quad \frac{\partial \rho}{\partial x} = \frac{\rho_R g}{a^2}\frac{\partial H}{\partial x}.$$

It follows that Eq. (2.14) has the form

$$\frac{\partial H}{\partial t} + u\frac{\partial H}{\partial x} + \frac{a^2}{g}\frac{\rho}{\rho_R}\frac{\partial u}{\partial x} = 0,$$

which reduces to Eq. (2.7) when $\rho \equiv \rho_R$ provided the acoustic velocity is given by Eq. (2.8). In the same way, we find that Eq. (2.15) has the form

$$\frac{\partial u}{\partial t} + u\frac{\partial u}{\partial x} + \frac{\rho_R}{\rho} g\frac{\partial H}{\partial x} + \frac{fu|u|}{2D} = 0,$$

which is Eq. (2.10) when $\rho \equiv \rho_R$.

The characteristics of Eqs. (2.14) and (2.15) are

$$\lambda = G/\rho \pm a \quad (= u \pm a),$$

and the characteristic forms for the system are

$$\left.\begin{aligned} &\text{a)}\quad \frac{dx}{dt} = G/\rho + a \\ &\text{b)}\quad (a - G/\rho)\frac{d\rho}{dt} + \frac{dG}{dt} + \frac{fG|G|}{2\rho D} = 0 \end{aligned}\right\} \text{ on } C^{+} \tag{8.1}$$

$$\left.\begin{aligned} &\text{a)}\quad \frac{dx}{dt} = G/\rho - a \\ &\text{b)}\quad -(a + G/\rho)\frac{d\rho}{dt} + \frac{dG}{dt} + \frac{fG|G|}{2\rho D} = 0 \end{aligned}\right\} \text{ on } C^{-} \tag{8.2}$$

In order to obtain the benchmark values we use the method of characteristics with linear interpolation. The finite difference approximations of these equations is the same as described in section 3 for the case of linear interpolation.

## 9. THE TWO-STEP LAX-WENDROFF DIFFERENCE SCHEME

The two-step Lax-Wendroff scheme (cf. [7], [8]) is one of the most popular methods for solving compressible flow problems. It is an explicit two-step method based on a second order Taylor series expansion in time; thereby generating second order accuracy in time. When applied to systems of hyperbolic equations in conservative form, the scheme can be described as follows. Let us consider the system

$$\frac{\partial w}{\partial t} + \frac{\partial}{\partial x} B(x,t,w) = F(x,t,w) \tag{9.1}$$

where $w = w(x,t)$ is a vector valued function of the spatial variable $x$ and time $t$, and $B$ and $F$ are vector valued functions of the indicated arguments. Let $0 = x_1 < x_2 < \ldots < x_{N+1} = L$ denote a mesh on the interval $[0,L]$, and $\{t^n\}_{n=1}$ a sequence of time values. Set $w_j^n = w(x_j,t^n)$, $B_j^n = B(x_j,t^n,w_j^n)$, and $F_j^n = F(x_j,t^n,w_j^n)$. Let the mesh have equal spacing $\delta x = x_j - x_{j-1}$, and set $\delta t^n = t^{n+1} - t^n$, then given $\{w_j^n\}$ the procedure consists of two steps. The first step involves the use of the Lax method to obtain intermediate values associated with the points $(x_{j\pm\frac{1}{2}}, t^{n+\frac{1}{2}})$ as shown in Fig. 9.1. The second step involves the use of a forward time step from $t^n$ to $t^{n+1}$ with a space centered difference approximation using the intermediate values from the first step.

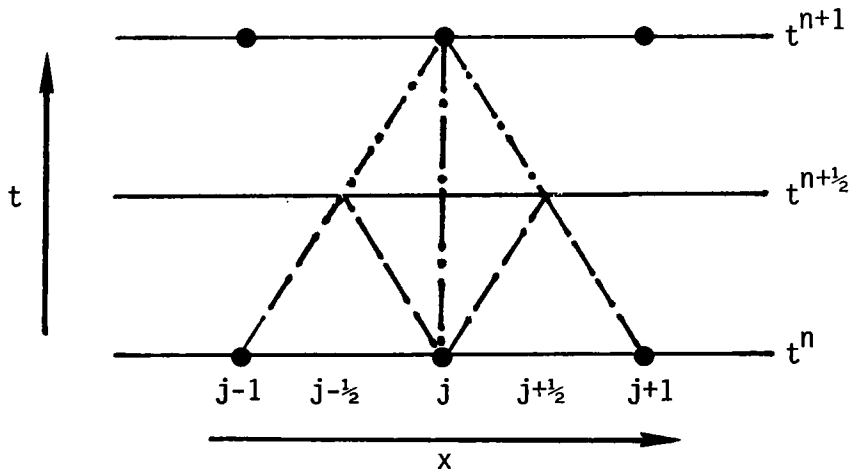


Fig. 9.1 A Portion of Grid for Lax-Wendroff Scheme

For a system of the form (9.1), the first step in finding $w_j^{n+1}$ will be to calculate the intermediate values

$$\begin{aligned} w_{j-\frac{1}{2}}^{n+\frac{1}{2}} &= \frac{1}{2}(w_{j-1}^n + w_j^n) - \frac{\delta t^n}{2\delta x}(B_j^n - B_{j-1}^n) + \frac{\delta t^n}{2}\frac{1}{2}(F_{j-1}^n + F_j^n) , \\ w_{j+\frac{1}{2}}^{n+\frac{1}{2}} &= \frac{1}{2}(w_j^n + w_{j+1}^n) - \frac{\delta t^n}{2\delta x}(B_{j+1}^n - B_j^n) + \frac{\delta t^n}{2}\frac{1}{2}(F_j^n + F_{j+1}^n) . \end{aligned} \tag{9.2}$$

Then define

$$\begin{aligned} B_{j\pm\frac{1}{2}}^{n+\frac{1}{2}} &= B(x_{j\pm\frac{1}{2}},\ t^{n+\frac{1}{2}},\ w_{j\pm\frac{1}{2}}^{n+\frac{1}{2}}) , \\ F_{j\pm\frac{1}{2}}^{n+\frac{1}{2}} &= F(x_{j\pm\frac{1}{2}},\ t^{n+\frac{1}{2}},\ w_{j\pm\frac{1}{2}}^{n+\frac{1}{2}}) . \end{aligned} \tag{9.3}$$

The second step is then given by

$$w_j^{n+1} = w_j^n - \frac{\delta t^n}{\delta x}(B_{j+\frac{1}{2}}^{n+\frac{1}{2}} - B_{j-\frac{1}{2}}^{n+\frac{1}{2}}) + \frac{\delta t^n}{2}(F_{j+\frac{1}{2}}^{n+\frac{1}{2}} - F_{j-\frac{1}{2}}^{n+\frac{1}{2}}) . \tag{9.4}$$

Difference Equations

In our application, $w = (\rho, G)'$, and from (2.5) and (2.13c) we have

$$\frac{\partial \rho}{\partial x} = \rho_R g \frac{\partial H}{\partial x} = a^2 \frac{\partial \rho}{\partial x} ;$$

thus $B = (G,\ G^2/\rho + a^2\rho)$, and $F = (0,\ -fG|G|/2D\rho)$. Relative to the $j^{th}$ mesh point, the first step takes the form

$$\text{a)} \quad \rho_{i-\frac{1}{2}}^{n+\frac{1}{2}} = \frac{1}{2}(\rho_{i-1}^n + \rho_i^n) - \frac{\delta t^n}{2\delta x}(G_i^n - G_{i-1}^n) , \tag{9.5}$$

$$\begin{aligned} \text{b)} \quad G_{i-\frac{1}{2}}^{n+\frac{1}{2}} &= \frac{1}{2}(G_{i-1}^n + G_i^n) - \frac{\delta t^n}{2\delta x}\left[(G_i^n)^2/\rho_i^n - (G_{i-1}^n)^2/\rho_{i-1} + a^2(\rho_i^n - \rho_{i-1}^n)\right] \\ &\quad - \frac{\delta t^n f}{8D}\left[G_i^n|G_i^n|/\rho_i^n + G_{i-1}^n|G_{i-1}^n|/\rho_{i-1}^n\right] , \quad \text{for } i=j,j+1 . \end{aligned}$$

The second step takes the form

$$\begin{aligned} \text{a)} \quad & \rho_j^{n+1} = \rho_j^n - \frac{\delta t^n}{\delta x}\left(G_{j+\frac{1}{2}}^{n+\frac{1}{2}} - G_{j-\frac{1}{2}}^{n+\frac{1}{2}}\right) \\ \text{b)} \quad & G_j^{n+1} = G_j^n - \frac{\delta t^n}{\delta x}\left[\left(G_{j+\frac{1}{2}}^{n+\frac{1}{2}}\right)^2/\rho_{j+\frac{1}{2}}^{n+\frac{1}{2}} - \left(G_{j-\frac{1}{2}}^{n+\frac{1}{2}}\right)^2/\rho_{j-\frac{1}{2}}^{n+\frac{1}{2}} + a^2\left(\rho_{j+\frac{1}{2}}^{n+\frac{1}{2}} - \rho_{j-\frac{1}{2}}^{n+\frac{1}{2}}\right)\right] \\ & \quad - \frac{\delta t^n f}{4D}\left[G_{j+\frac{1}{2}}^{n+\frac{1}{2}}\left|G_{j+\frac{1}{2}}^{n+\frac{1}{2}}\right|/\rho_{j+\frac{1}{2}}^{n+\frac{1}{2}} + G_{j-\frac{1}{2}}^{n+\frac{1}{2}}\left|G_{j-\frac{1}{2}}^{n+\frac{1}{2}}\right|/\rho_{j-\frac{1}{2}}^{n+\frac{1}{2}}\right] . \end{aligned} \tag{9.6}$$

The time step $\delta t^n$ is selected, as before, using the Courant condition

$$\delta t^n \leq \delta x/(a + |u^n|) , \tag{9.7}$$

where $|u^n| = \max\{|G_j^n|/\rho_j^n: 1 \leq j \leq N+1\}$. In practice equality is used in (9.7).

Boundary Conditions

The two-step Lax-Wendroff is applicable at the interior points but not at the boundary. Since, for a fixed ratio $\delta t/\delta x$, the scheme is asymptotically second order in $\delta t$, the treatment at the boundaries should attempt to maintain this accuracy. To achieve this accuracy at the boundaries, we have used the method of characteristics. The procedure can be described as follows.

Left Boundary

On the left boundary we use the characteristic equation associated with the $C^-$ curve defined in Eq. (8.2). Thus on $C^-$, we have

$$\begin{aligned} \text{a)} \quad & \frac{dx}{dt} = G/\rho - a , \\ \text{b)} \quad & -(a + G/\rho)\frac{d\rho}{dt} + \frac{dG}{dt} + \frac{fG|G|}{2\rho D} = 0 . \end{aligned} \tag{9.8}$$

Using the approximations described in section 3, with linear interpolation, we find

$$\begin{aligned} \text{a)} \quad & \rho_1^{n+1} = \rho_{OR} , \\ \text{b)} \quad & G_1^{n+1} = (a+u_s)\rho_{OR} - a\rho_s - \delta t^n f\, G_s|G_s|/2D\rho_s , \end{aligned} \tag{9.9}$$

where

$$\begin{aligned} &\text{a)} \quad u_s = \left[u_1^n + a\alpha(u_2^n - u_1^n)\right] \Big/ \left[1 + \alpha(u_2^n - u_1^n)\right] , \\ &\text{b)} \quad \rho_s = \rho_{OR} + \alpha(a - u_s)(\rho_2^n - \rho_{OR}) , \\ &\text{c)} \quad G_s = \rho_s u_s , \\ &\text{d)} \quad \alpha = \delta t^n / \delta x . \end{aligned} \tag{9.10}$$

Right Boundary

At the right boundary, we use the $C^+$ characteristic Eqs. (8.1) which, after differencing with linear interpolation, take the form

$$(a - u_c)\rho_{N+1}^{n+1} + G_{N+1}^{n+1} = (a - u_c)\rho_c + G_c - \delta t^n f G_c |G_c| / 2D\rho_c = Z_c , \tag{9.11}$$

where

$$\begin{aligned} &\text{a)} \quad u_c = \left[u_{N+1}^{n+1} + \alpha a(u_N^n - u_{N+1}^n)\right] \Big/ \left[1 + \alpha(u_{N+1}^n - u_N^n)\right] , \\ &\text{b)} \quad \rho_c = \rho_{N+1}^n + \alpha(a + u_c)(\rho_N^n - \rho_{N+1}^n) , \\ &\text{c)} \quad G_c = \rho_c u_c , \\ &\text{d)} \quad \alpha = \delta t^n / \delta x . \end{aligned} \tag{9.12}$$

The boundary condition (2.17) is written in the form

$$G_{N+1}^{n+1} = u_0 \tau(t) \rho_{N+1}^{n+1} \left[a^2 \rho_{N+1}^{n+1} / \rho_R g H_0 - C_R / H_0\right]^{\frac{1}{2}} . \tag{9.13}$$

If we set $\rho = \rho_{N+1}^{n+1}$, $G = G_{N+1}^{n+1}$, $c_1 = u_0 \tau(t)$, $c_2 = a^2 / \rho_R g H_0$, and $c_3 = c_R / H_0$; Eqs. (9.11) and (9.13) have the form

$$\begin{aligned} &\text{a)} \quad (a - u_c)\rho + G = Z_c \\ &\text{b)} \quad G = c_1 \rho \left[c_2 \rho - c_3\right]^{\frac{1}{2}} \end{aligned} \tag{9.14}$$

or

$$f(\rho) = (a - u_c)\rho + c_1 \rho \left[c_2 \rho - c_3\right]^{\frac{1}{2}} - Z_c = 0 . \tag{9.15}$$

This equation is solved using the Newton-Raphson iterations

$$\rho^{(\ell+1)} = \rho^{(\ell)} - f(\rho^{(\ell)})/f'(\rho^{(\ell)}) \tag{9.16}$$

with

$$\begin{aligned} &\text{a)} \quad \rho^{(0)} = \rho_{N+1}^{(n)}, \quad \text{and} \\ &\text{b)} \quad f'(\rho) = a + u_c + \left[c_1(3c_2\rho - 2c_3)/2(c_2\rho - c_3)^{\frac{1}{2}}\right] . \end{aligned} \tag{9.17}$$

The iterations are stopped when

$$\left|1 - \rho^{(\ell+1)}/\rho^{(\ell)}\right| < 10^{-9} \; ; \tag{9.18}$$

whereupon

$$\rho_{N+1}^{n+1} = \rho^{(\ell+1)} \; . \tag{9.19}$$

The two-step Lax-Wendroff scheme in this study used the method of characteristic treatment at the boundaries, and (9.5),(9.6) at the interior points.

## 10. DONOR CELL TYPE DIFFERENCE METHOD

A well known and very popular difference method for conservative form flow is the donor cell difference technique ([5],[7],[16],[17]). In fact, it is not a single technique but rather a general approach to differencing flow equations. Since there are so many variants of this general technique, we shall not ascribe the difference method described herein to any one source. Rather, we claim that it represent one example of this general technique.

### Difference Equations

We start from the system (2.14) and (2.15) which we write in the following form.

$$\frac{\partial \rho}{\partial t} + \frac{\partial}{\partial x}(\rho u) = 0 \tag{10.1}$$

$$\frac{\partial G}{\partial t} + \frac{\partial}{\partial x}(uG) = -\frac{\partial p}{\partial x} - fG|G|/2D\rho - \rho g \tag{10.2}$$

Let the interval $[0,L]$ be subdivided by an equally spaced mesh where $\pi$: $0 = x_1 < x_2 < \ldots < x_{N+1} = L$. The primary variables $\rho$ and G will be centered differently on the mesh. That is,

$$\begin{aligned} &\text{a)} \quad \rho_i^n \doteq \rho(x_{i+\frac{1}{2}}, t^n) \ , \\ &\text{b)} \quad G_i^n \doteq G(x_i, t^n) \ , \end{aligned} \tag{10.3}$$

where $x_{i+\frac{1}{2}} = \frac{1}{2}(x_i + x_{i+1})$. Thus we associate $\rho_i^n$ with the center of the cell $[x_i, x_{i+1}]$, and $G_i^n$ is associated with the edge $x_i$. The secondary variables $u_i^n$ and $H_i^n$ are defined as follows.

$$\begin{aligned} &\text{a)} \quad u_i^n = G_i^n/\bar{\rho}_i^n \ , \text{ where } \bar{\rho}_i^n = \tfrac{1}{2}(\rho_{i-1}^n + \rho_i^n) \ , \text{ and} \\ &\text{b)} \quad H_i^n = a^2 \rho_i^n/\rho_R g - c_R \ . \end{aligned} \tag{10.4}$$

In general the overbar on any variable will denote an arithmetic average for that variable, e.g. $\bar{u}_i^n = \frac{1}{2}(u_{i-1}^n + u_1^n)$. One feature of donor cell differencing is to maintain the conservative property of the original differential equations.

To this end, the continuity and momentum equations are each integrated over a control volume. For the continuity equation, the control volume is $[x_i, x_{i+1}]$; whereas for the momentum equation, the control volume is $[x_{i-\frac{1}{2}}, x_{i+\frac{1}{2}}]$.

Integrate the continuity equation over the interval $[x_i, x_{i+1}]$ obtaining

$$\frac{\partial}{\partial t}\left(\int_{x_i}^{x_{i+1}} \rho\right) + (\rho u)_{i+1} - (\rho u)_i = 0 \ . \tag{10.5}$$

We make the approximate

$$\frac{\partial}{\partial t}\left(\int_{x_i}^{x_{i+1}} \rho\right) \cong \delta x \, \frac{\partial}{\partial t} \rho_i \ , \tag{10.6}$$

recall that $\rho_i \triangleq \rho(x_{i+\frac{1}{2}}, t)$. In advancing from $t^n$ to $t^{n+1}$ we shall use single step time differencing; thus:

$$\frac{\partial}{\partial t} \rho_i \cong (\rho_i^{n+1} - \rho_i^n)/\delta t^n \ . \tag{10.7}$$

Donor cell averaging is used on the quantities $(\rho u)_{i+1}$ and $(\rho u)_i$. This is defined as follows: Let $0 \leq \theta \leq 1$ be given, and set

$$\begin{aligned} \theta_i &= \theta \ \mathrm{sign}(u_i), \quad \text{and} \\ \langle \rho \rangle_i &= \frac{1}{2}\left[(1+\theta_i)\rho_{i-1} + (1-\theta_i)\rho_i\right] \ . \end{aligned} \tag{10.8}$$

Then we set:

$$(\rho u)_i = \langle \rho \rangle_i \, u_i \ . \tag{10.9}$$

When $\theta = 1$ this is the usual upwind differencing (cf. [7]), and when $\theta = 0$ this is central differencing. Combining the approximations in (10.6-7), using (10.9), and considering an explicit scheme, we obtain the following difference approximation to the continuity equation, with $\alpha = \delta t^n/\delta x$,

$$\rho_i^{n+1} = \rho_i^n - \alpha\left[\langle \rho \rangle_{i+1}^n u_{i+1}^n - \langle \rho \rangle_i^n u_i^n\right] \ . \tag{10.10}$$

For the momentum equation, we integrate over $[x_{i-\frac{1}{2}}, x_{i+\frac{1}{2}}]$

$$\frac{\partial}{\partial t}\left(\int_{x_{i-\frac{1}{2}}}^{x_{i+\frac{1}{2}}} G\right) + (uG)_{i+\frac{1}{2}} - (uG)_{i-\frac{1}{2}} = -(P_i - P_{i-1}) - \int_{x_{i-\frac{1}{2}}}^{x_{i+\frac{1}{2}}} fG|G|/2D\rho. \quad (10.11)$$

Again we are interested in single time step approximations; thus

$$\frac{\partial}{\partial t}\left(\int_{x_{i-\frac{1}{2}}}^{x_{i+\frac{1}{2}}} G\right) \cong \frac{\delta x}{\delta t^n}\,(G_i^{n+1} - G_i^n)\ . \quad (10.12)$$

For the moment we are interested in explicit schemes; thus we will use the following approximation.

$$\int_{x_{i-\frac{1}{2}}}^{x_{i+\frac{1}{2}}} fG|G|/2D\rho \cong \delta x f G_i^n |G_i^n|/2D\bar{\rho}_i^n\ . \quad (10.13)$$

Donor cell averaging is used on the quantities $(uG)_{i+\frac{1}{2}}$ and $(uG)_{i-\frac{1}{2}}$. Define

$$\begin{aligned} &\text{a)} \quad \theta_{i+\frac{1}{2}} = \theta\ \text{sign}\left[(u_i^n + u_{i+1}^n)/2\right]\ , \\ &\text{b)} \quad \langle G\rangle_{i+\frac{1}{2}}^n = \frac{1}{2}\left[(1+\theta_{i+\frac{1}{2}})G_i^n + (1-\theta_{i+\frac{1}{2}})G_{i+1}^n\right]\ . \end{aligned} \quad (10.14)$$

Then we use the approximation

$$(uG)_{i+\frac{1}{2}} \cong \langle G\rangle_{i+\frac{1}{2}}^n\ \bar{u}_{i+\frac{1}{2}}^n\ , \quad (10.15)$$

where $\bar{u}_{i+\frac{1}{2}}^n = \frac{1}{2}(u_i^n + u_{i+1}^n)$. With these approximations, Eq. (10.11) takes the following form.

$$\begin{aligned} G_i^{n+1} = G_i^n - \alpha\Big[&\langle G\rangle_{i+\frac{1}{2}}^n\ \bar{u}_{i+\frac{1}{2}}^n - \langle G\rangle_{i-\frac{1}{2}}^n\ \bar{u}_{i-\frac{1}{2}}^n + \rho_R g(H_i^n - H_{i-1}^n)\Big] \\ &- \delta t^n f\ G_i^n|G_i^n|/2D\bar{\rho}_i^n\ . \end{aligned} \quad (10.16)$$

Equations (10.10) and (10.16) are the basic donor cell difference equations at the interior point. In principle, these equations are conditionally stable, i.e. if $\alpha = \alpha_n = \delta t^n/\delta x$ is suitably restricted. We shall see, however, that for water hammer equations where $|u| \ll a$, stability can be achieved only when $\alpha$ is severely restricted. Indeed, it has been shown (cf. [18],[7] p. 238) that the stability restriction for inviscid flow with heat conduction in two

dimensions given by

$$\delta t^n \leq \frac{(|u| + |v|)\delta x}{(|u| + |v| + a\sqrt{2})^2} .$$

Clearly, when $|u|, |v| \ll a$, this criterion imposes a severe restriction on the time steps.

For this reason we have modified Eq. (10.16) by making the pressure term implicit in time rather than explicit. Thus we use $(H_i^{n+1} - H_{i-1}^{n+1})$ in (10.16) and solve the resulting system by iterations on the pressure. This procedure is similar to that employed by Amsden and Hirt in the YAQUI code [19]. The iterative procedure is

$$\begin{aligned}
\hat{\rho}_i^{(\ell)} &= \rho_i^n - \alpha\left[\langle\hat{\rho}\rangle_{i+1}^{(\ell-1)} u_{i+1}^n - \langle\hat{\rho}\rangle_i^{(\ell-1)} u_i^n\right] , \\
\hat{H}_i^{(\ell)} &= a^2\hat{\rho}^{(\ell)}/\rho_R g - CR , \\
\hat{G}_i^{(\ell)} &= G_i^n - \alpha\Big[\langle G\rangle_{i+\frac{1}{2}}^n \bar{u}_{i+\frac{1}{2}}^n - \langle G\rangle_{i-\frac{1}{2}}^n \bar{u}_{i-\frac{1}{2}}^n \\
&\qquad + \rho_R g(\hat{H}_i^{(\ell)} - \hat{H}_{i-1}^{(\ell)})\Big] - \delta t^n f G_i^n |G_i^n| / 2D\bar{\rho}_i^n , \\
\hat{u}_i^{(\ell)} &= \hat{G}_i^{(\ell)}/\overline{\hat{\rho}_i^{(\ell)}}
\end{aligned} \qquad (10.17)$$

where $\hat{\rho}_i^{(0)} = \rho_i^{n-1}$, $\hat{u}_i^{(0)} = u_i^{n-1}$, $\hat{G}_i^{(0)} = G_i^{n-1}$ .

In this study we used $\ell = 2$ in these iterations so that $\rho_i^{n+1} = \hat{\rho}_i^{(2)}$ and $G_i^{n+1} = \hat{G}_i^{(2)}$. Using one corrective iteration in this way raised the stability criterion from a very small value to a value near the usual Courant condition. That is, let $\alpha_0 = 1/(a+|u^n|)$ where $|u^n| = \max\{|u_i^n| : 1 \leq i \leq N+1\}$, then the usual Courant condition is $\alpha = \delta t^n/\delta x \leq \alpha_0$ with equality generally used. With the explicit donor cell method (no iterations) we found $\alpha/\alpha_0 \ll 1$; whereas with two corrective iterations $\alpha/\alpha_0$ is near one.

## Boundary Conditions

Recall that at the left boundary the density is specified by

$$\rho(0,t^n) \equiv \rho_{\frac{1}{2}}^n \equiv \rho_{0R} .$$

Thus it remains to determine $G_1^n$ at the left boundary. Recall that in deriving the approximation to the momentum equation, the first interval used in the integration was $[x_{3/2},x_{5/2}]$; thus we have the half interval $[x_1,x_{3/2}]$ which has not been accounted for in this process. We could derive an equation for $G_1^{n+1}$ by integrating the momentum equation over this half interval. Alternatively, we could append a fictitious interval to the left of the boundary, extrapolate to obtain values of the variables in this interval, and then use the donor cell difference technique to obtain the appropriate equation. This latter approach is in the spirit of donor cell differencing and we shall use this approach at the boundaries. To this end, we append a mesh cell $[x_0,x_1]$ with $x_0 = -\delta x$ ($x_1 = 0$) to the original mesh, and use linear extrapolation to define $G_0^n$ and $\rho_0^n$ (note $\rho_0^n \sim \rho(x_{\frac{1}{2}},t^n)$ is associated with the midpoint of this extra cell). Applying Eq. (10.16) for $i = 1$, we then find

$$G_1^{n+1} = G_1^n - \alpha\left[\langle G\rangle_{3/2}^n \bar{u}_{3/2}^n - \langle G\rangle_{\frac{1}{2}}^n \bar{u}_{\frac{1}{2}}^n + \rho_R g(H_1^n - H_0^n)\right] - \delta t^n f G_1^n |G_1^n|/2D\bar{\rho}_1^n \,. \tag{10.18}$$

This equation is written in its explicit form although in practice a corrective iteration is done with this equation just as with the interior equations.

At the right boundary, we again append an additional mesh cell $[x_{N+1},x_{N+2}]$ on the right with $x_{N+2} = L+\delta x$, extrapolate the variables to this cell, and apply the donor cell differencing method to the momentum equation. We find

$$G_{N+1}^{n+1} = G_{N+1}^n - \alpha\left[\langle G\rangle_{N+3/2}^n \bar{u}_{N+3/2}^n - \langle G\rangle_{N+\frac{1}{2}}^n \bar{u}_{N+\frac{1}{2}}^n + \rho_R g(H_{N+1}^{n+1} - H_N^{n+1})\right] - \delta t^n f G_{N+1}^n |G_{N+1}^n|/2D\rho_{N+\frac{1}{2}}^n \,. \tag{10.19}$$

There are several aspects of this equation that are worth noting. First, it is implicit since we are using $H_{N+1}^{n+1} - H_N^{n+1}$. This is because we have to use an implicit technique on the right boundary regardless of what we do at the interior points. All methods studied in this report treat the right boundary in an implicit manner. If $H_{N+\frac{1}{2}}$ denotes the boundary value for the pressure head, then the boundary condition on the right is

$$G_{N+1}^{n+1} = u_0\tau(t)\rho_{N+\frac{1}{2}}^{n+1}\left[H_{N+\frac{1}{2}}^{n+1}/H_0\right]^{\frac{1}{2}} . \tag{10.20}$$

We use Eq. (10.20) in Eq. (10.19), observe that $H_{N+1}^{n+1}-H_N^{n+1} = 2(H_{N+\frac{1}{2}}^{n+1}-H_N^{n+1})$, and note that $H_{N+\frac{1}{2}}^{n+1} = a^2\rho_{N+\frac{1}{2}}^{n+1}/\rho_R g - C_R$. We then wish to solve the equation

$$f(\rho) = c_1\rho\left[c_2\rho-c_3\right]^{\frac{1}{2}} + 2\alpha\rho_R g(c_2\rho-c_3) - z = 0 \tag{10.21}$$

where

$$\begin{aligned}
&\text{a)} \quad c_1 = u_0\tau(t) , \\
&\text{b)} \quad c_2 = a^2/\rho_R g H_0 , \\
&\text{c)} \quad c_3 = c_R/H_0 , \\
&\text{d)} \quad z = G_{N+1}^n - \alpha\left[\langle G\rangle_{N+3/2}^n \bar{u}_{N+3/2}^n - \langle G\rangle_{N+\frac{1}{2}}^n \bar{u}_{N+\frac{1}{2}}^n - \rho_R g H_N^{n+1}\right] \\
&\qquad\qquad - \delta t^n f\, G_{N+1}^n |G_{N+1}^n|/2D\rho_{N+\frac{1}{2}}^n .
\end{aligned} \tag{10.22}$$

This equation is solved with Newton-Raphson iterations to obtain $\rho_{N+\frac{1}{2}}^{n+1}$. Then we set

$$G_{N+1}^{n+1} = c_1\rho_{N+\frac{1}{2}}^{n+1}\left[c_2\rho_{N+\frac{1}{2}}^{n+1}-c_3\right]^{\frac{1}{2}} . \tag{10.23}$$

to complete the calculation at the right boundary.

## 11. COMPARISON OF THE METHOD OF CHARACTERISTICS, TWO-STEP LAX-WENDROFF, AND DONOR CELL TYPE DIFFERENCING

In this section we compare approximations to the rigid wall model with the conservative governing Eqs. (3.1). In the case of the rigit wall model governed by the system (2.14) and (2.15), the primary dependent variables are $(\rho,G)$; whereas in the elastic wall model, the primary variables were $(u,H)$. For purposes of comparison with the elastic wall model (we may note here the comparison is valid only if $\rho = \rho_R$ and the acoustic speed has the same value in both models), we have used the following relations: $u = G/\rho$ and $H = a^2\rho/\rho_R g - c_R$ (cf. Eq. (2.13c)). Thus all numerical results will be presented in terms of the velocity u and the pressure head H. In this section we have restricted our attention to the case of m = 1. Moreover, when presenting numerical results, our attention will be focused as before at the time t = 7.728 and on the velocity at this time.

### Benchmark Values

For this study the benchmark values are determined by the method of characteristics with N = 80 and linear interpolation. To highlight the differences if any between the rigid wall $(\rho,G)$ model and the elastic wall $(u,H)$ model, it is worth comparing the benchmark values for the two models. To this end, Table 11.1 presents the velocities at t = 7.728 and at selected points $\bar{x}$ = 0, 0.2, 0.4, 0.6, and 0.8 along the pipe.

TABLE 11.1 Comparison of Benchmark Values

| $\bar{x} = x/L$ | $(\rho,G)$ model Linear Interpolation N = 80 | $(u,H)$ model Linear Interpolation N = 80 | $(u,H)$ model Quadratic Interpolation N = 80 |
|---|---|---|---|
| 0.0 | -0.291567 | -0.291590 | -0.291594 |
| 0.2 | -0.290154 | -0.290176 | -0.290428 |
| 0.4 | -0.268600 | -0.268617 | -0.268613 |
| 0.6 | -0.249244 | -0.249254 | -0.249251 |
| 0.8 | -0.161366 | -0.161371 | -0.161368 |

From this table we conclude that the numerical differences between these two models are negligible for the purposes of this study. Thus the numerical results presented in section 7 can be directly compared with the numerical results in this section. However, in this section we have selected the $(\rho,G)$ model with linear interpolation and N = 80, as the benchmark, for the sake of consistency.

Donor Cell Differencing Method

The donor cell technique which we have considered consists of two versions -- an explicit version and the version with two iterative corrections which we will refer to as the quasi iterative version. Each version has three parameters associated with it. The first is the number of mesh cells N which is also the number of variables associated with each dependent variable. The second parameter is $\theta$ which determines the donor cell averaging as discussed in section 10. (Recall that $\theta = 0$ corresponds to central differencing whereas $\theta = 1$ corresponds to upwind differencing.) The third parameter is the time step size which we measure in terms of the Courant step. That is, we set $\alpha_0 = 1/(a + |\bar{u}^n|)$, $\alpha = \delta t^n/\delta x$ and use the ratio $\alpha/\alpha_0$ as a measure of the step size. Thus $\alpha/\alpha_0 = 1$ is taken as the norm for an explicit method. Before comparing the donor cell technique with other methods we shall select one version and for this version we shall select appropriate values for $\theta$ and $\alpha/\alpha_0$.

We first compare the explicit version and the quasi-iterative version with respect to the stability limit. That is, both versions are conditionally stable in the sense that for $\alpha/\alpha_0$ sufficiently small, the method is stable. We determine whether a method is stable or not by examining the velocity profile near the end of the transient at t = 7.728. If the method is stable, this profile is monotonic.

For the explicit version of the donor cell technique we set $\theta = 1$ (upwind differencing) since we would expect this value of $\theta$ to provide the most stable scheme, i.e. the largest stability limit. We then check for stability with various values for the ratio $\alpha/\alpha_0$ with N = 5 and 10. The results are presented in Table 11.2. In this table we have also shown the number of time steps (which is determined by the size of $\alpha/\alpha_0$) needed to reach t = 7.728.

TABLE 11.2 Stability Limits for Explicit Donor Cell Method, $\theta = 1$

| $\alpha/\alpha_0$ | N = 5 | | N = 10 | |
|---|---|---|---|---|
| | Stable | # Time Steps | Stable | # Time Steps |
| 1.0 | No | 47 | No | 83 |
| 0.1 | No | 371 | No | 728 |
| 0.05 | Yes | 739 | No | 1451 |
| 0.025 | Yes | --- | Yes | 2890 |

From this table it is clear that the explicit version is not practical for solving waterhammer problems of the type considered in this study. In Table 11.3, we present stability results for the quasi-iterative version of the donor cell method. The results in this table are the same for $\theta = 0.0$ or 1.0.

TABLE 11.3 Stability Limits for Quasi-Iterative Method, $\theta = 1.0$ or 0.0

| $\alpha/\alpha_0$ | N = 5 | | N = 10 | | N = 20 | | N = 40 | |
|---|---|---|---|---|---|---|---|---|
| | Stable | # Time Steps | Stable | # Time Steps | Stable | # Time Steps | Stable | # Time Steps |
| 1.0 | No | 47 | No | 83 | No | 155 | No | 299 |
| 0.9 | No | 50 | No | 96 | Yes | 164 | No | 326 |
| 0.8 | No | 54 | Yes | 101 | Yes | --- | Yes | 371 |
| 0.7 | Yes | 56 | Yes | --- | Yes | --- | Yes | --- |

Table 11.3 shows that the quasi-iterative version of the donor cell method is at least a viable technique in contrast to the explicit donor cell method.

It should be noted that the stability limit appeared to be independent of the number of corrective iterations. For this reason we selected two

iterations for this study. From this point on we shall consider only the quasi-iterative version.

We now consider the selection of the donor cell averaging parameters. To this end we set N = 10 in the quasi-iterative version, $\alpha/\alpha_0 = 0.8$ and compared the velocities at t = 7.728 for $\theta = 0.0$, 0.5, and 1.0. The results are shown in Table 11.4.

TABLE 11.4 Comparison of Accuracy in Velocity at t = 7.728 and Spatial Points $\bar{x}$ for $\theta = 0.0, 0.5, 1.0$

| $\bar{x} = x/L$ | $\theta = 0.0$ | | $\theta = 0.5$ | | $\theta = 1.0$ | |
|---|---|---|---|---|---|---|
| | velocity | % r.e. | velocity | % r.e. | velocity | % r.e. |
| 0.0 | -0.296360 | 1.64 | -0.296336 | 1.64 | -0.296312 | 1.63 |
| 0.2 | -0.291229 | 0.37 | -0.291227 | 0.37 | -0.291224 | 0.37 |
| 0.4 | -0.255267 | 4.96 | -0.255281 | 4.96 | -0.255294 | 4.95 |
| 0.6 | -0.267553 | 7.35 | -0.267489 | 7.32 | -0.267426 | 7.30 |
| 0.8 | -0.163697 | 1.45 | -0.163648 | 1.41 | -0.163670 | 1.43 |

From this table we conclude that there is no essential difference in the results for $\theta = 0.0$, 0.5, and 1.0. We shall arbitrarily select $\theta = 0.0$ when comparing with the other methods.

In summary, we have selected the quasi-iterative version (two corrective iterations) with $\theta = 0.0$ and $\alpha/\alpha_0 = 0.8$ as the representative donor cell method for comparison with the other methods.

## Comparison of the Three Methods

We now compare the accuracy of the three methods under consideration, that is, the method of characteristics, two-step Lax-Wendroff, and the quasi-iterative donor cell method. The comparison will be on the basis of the accuracy in the velocity at t = 7.728 for various choices of N. In Table 11.5 we display the maximum and the mean relative per cent error over the interior points (Int.) $\bar{x} = 0.2$, 0.4, 0.6, and 0.8. In addition, we also display the

TABLE 11.5 Comparison of Errors in the Velocity at t = 7.728

| | $\varepsilon_{max}$ | | | | | | $\varepsilon_{mean}$ | | |
|---|---|---|---|---|---|---|---|---|---|
| | N=5 | | N=10 | | N=20 | | N=5 | N=10 | N=20 |
| | Int. | Bnd. | Int. | Bnd. | Int. | Bnd. | Int. | Int. | Int. |
| Method of Characteristics (linear) | 2.9 | 0.36 | 0.39 | 0.33 | 0.31 | 0.15 | 1.6 | 0.17 | 0.10 |
| Two-Step Lax-Wendroff | 1.5 | 1.8 | 1.96 | 0.024 | 0.21 | 0.014 | 0.79 | 0.56 | 0.086 |
| Donor Cell $\theta$=0.0, $\alpha/\alpha_0$=.8 | 8.9* | 0.71* | 7.4 | 1.64 | 3.5 | 0.09 | 4.6* | 3.5 | 1.5 |

* $\alpha/\alpha_0$ = 0.7 for this case rather than $\alpha/\alpha_0$ = 0.8.

relative per cent error at the reservoir boundary (Bnd.). The results in this table can be compared directly with the corresponding results in Tables 7.2b and 7.3 - 7.5.

From Table 11.5, we conclude that the Two-Step Lax-Wendroff method (with method of characteristics used at the boundaries) has comparable accuracy with the method of characteristics. The donor cell method is clearly not of comparable accuracy. The proper treatment of boundary conditions is critical in obtaining accurate results. For example, in the two-step Lax-Wendroff method (which is second order accurate in time at the interior points), we tried techniques other than the method of characteristics at the boundary. In particular we tried the use of a fictitious mesh cell with extrapolation similar to that which was used in the donor cell method. In terms of accuracy, the Lax-Wendroff method fairs very poorly as shown in Table 11.6.

TABLE 11.6 Comparison of Treatment of Boundary Conditions with Two-Step Lax-Wendroff Method

| Boundary Treatment | $\varepsilon_{max}$ | | | | | | $\varepsilon_{mean}$ | | |
|---|---|---|---|---|---|---|---|---|---|
| | N=5 | | N=10 | | N=20 | | N=5 | N=10 | N=20 |
| | Int. | Bnd. | Int. | Bnd. | Int. | Bnd. | Int. | Int. | Int. |
| Method of Characteristics | 1.5 | 1.8 | 1.96 | 0.24 | 0.21 | 0.014 | 0.79 | 0.56 | 0.086 |
| Lax-Wendroff Extrapolation | 32.0 | 15.0 | 14.1 | 1.6 | 7.4 | 1.3 | 18.2 | 6.0 | 2.4 |

We have always tried to use the largest time steps possible, subject to the stability criterion imposed for any particular method. It might be supposed that additional accuracy could be gained by reducing the time step below the stability limit. However, most of the methods discussed in this study have numerical diffusion associated with them which increases as the time step is reduced. We illustrate this situation with the donor cell method for N = 5, $\theta$ = 0.0 and $\alpha/\alpha_0$ = 0.25, 0.5, and 0.7 where 0.7 is near the stability limit. The table 11.7 presents the maximum per cent relative error in the velocity at t = 7.728 for these three cases.

TABLE 11.7 Comparison of Accuracy for Three Time Step Sizes

| $\alpha/\alpha_0$ | $\varepsilon_{max}$ | # Time Steps |
|---|---|---|
| 0.7 | 8.9 | 56 |
| 0.5 | 16.9 | 83 |
| 0.25 | 20.6 | 155 |

## 12. CONCLUSIONS

In this study, we have compared the accuracy obtained with seven different approximations to a single pipe water hammer problem. In the following table we summarize the results for the accuracy of the seven methods. We have selected as before t = 7.728 and give the maximum relative per cent error in the velocity at the reservoir and the four interior points $\bar{x}$ = 0.2, 0.4, 0.6, and 0.8. From these results presented in Table 11.8, it is clear that from the point of view of accuracy, Two-Step Lax-Wendroff and the method of characteristics (both linear and quadratic) are comparable. The Lax method fairs worst. The donor cell and the Galerkin with quadratic B-splines give comparable accuracy, but the method of characteristics and two-step Lax-Wendroff methods clearly stand out, that is, produce the best accuracy.

TABLE 11.8 Comparison of Accuracy in the Velocity at t = 7.728

| | N = 5 | N = 10 | N = 20 |
|---|---|---|---|
| M.O.C. (Quad) | 1.95 | 2.1 | 0.18 |
| Two-Step Lax-Wendroff | 1.8 | 1.96 | 0.21 |
| M.O.C. (Linear) | 2.9 | 0.36 | 0.31 |
| Donor Cell ($\theta$=0.0, $\alpha/\alpha_0$=.8) | 8.9 | 7.4 | 3.5 |
| Galerkin (k=3, $\nu$=1) | 11.3 | 2.6 | 1.1 |
| Galerkin (k=2, $\nu$=1) | 23.8 | 5.4 | 1.9 |
| Lax | 50.9 | 14.9 | 4.9 |

ACKNOWLEDGMENT

The authors wish to express their gratitude to J. Beumer for her excellent typing as well as the preparation of many figures and tables appearing in this report.

# REFERENCES


[1] MacLaren, J. F. T., et al., A Comparison of Numerical Solutions of the Unsteady Flow Equations applied to Reciprocating Compressor Systems, J. Mech. Engng. Sci. 1975, 17, No. 5, pp. 271-279.

[2] Streeter, V. L. and Wylie, E. B., Hydraulic Transients, McGraw-Hill, New York, 1967.

[3] Courant, R. and Friedricks, K. O., Supersonic Flow and Shock Waves, Interscience Publ., New York, 1948.

[4] Courant, R., Friedricks, K., and Lewy, H., On Partial Difference Equations of Mathematical Physics, IBM Journal II, Mar 1967, pp. 215-234 (English trans. of the original. Uber die Portiellen Differenzengleichungen der Mathematischen Physik, Math. Annln, 1928, 100, 32-79).

[5] Hirt, C. W., Heuristic Stability Theory for Finite-Difference Equations, J. Comp. Physics, 2, 1968, pp. 339-355.

[6] Lax, P. D., Weak Solutions of Nonlinear Hyperbolic Equations and Their Numerical Computation, Comm. Pure & Appl. Math., 7, 1954, pp. 159-193.

[7] Roache, P. J., Computational Fluid Dynamics, Hermosa Publ., New Mexico, 1976.

[8] Potter, D., Computational Physics, J. Wiley & Sons, London, 1973.

[9] Oden, J. T., et al., eds., Finite Element Methods in Flow Problems, UAH Press, Huntsville, Alabama, 1974.

[10] Leaf, G., et al., DISPL: A Software Package for One and Two Spatially Dimensioned Kinetics-Diffusion Problems, Argonne National Laboratory Report ANL-77-12, May, 1977.

[11] Hindmarsh, A. C., GEARB: Solution of Ordinary Differential Equations Having Banded Jacobians, Lawrence Livermore Laboratory Report UCID-30059, Rev. 1, March 1975.

[12] De Boor, C., On Calculating with B-Splines, J. Approximation Theory, 6, 1972, pp. 50-62.

[13] De Boor, C., Package for Calculating with B-Splines, MRC Technical Summary Report, 1333, Math. Research Center, Univ. of Wisconsin, 1973.

[14] Steffensen, J. F., Interpolation, Chelsea Publishing Company, New York (1950).

[15] Strang, G. and Fix, G., An Analysis of the Finite Element Method, Prentice Hall, Inc., N.J. (1973).

[16] Tunstall, J. N., On the Derivation of Conservative Finite Difference Expressions for the Navier-Stokes Equations, Oak Ridge Gaseous Diffusion Plant Report K/CSD-5, April 1977.

[17] Hirt, C., Amsden, A., and Cook, J., An Arbitrary Lagrangian-Eulerian Computing Method for all Flow Speeds, J. Comp. Physics, 14 (1974), pp. 227-253.

# Distribution for ANL-77-81

Internal:

M. V. Nevitt
B. Ancker-Johnson
R. J. Royston
R. Avery
J. F. Marchaterre
H. K. Fauske
A. J. Goldman
D. Rose
E. L. Martinec
D. H. Lennox
D. R. Ferguson
G. K. Leaf (20)
T. C. Chawla (20)
P. L. Witkowski (10)
A. B. Krisciunas
ANL Contract Copy
ANL Libraries (5)
TIS Files (6)

External:

DOE-TIC, for distribution per UC-32 (203)
Manager, Chicago Operations Office
Chief, Chicago Patent Group
President, Argonne Universities Association
Applied Mathematics Division Review Committee:
  P. J. Eberlein, SUNY at Buffalo
  G. Estrin, U. California, Los Angeles
  W. M. Gentleman, U. Waterloo
  J. M. Ortega, North Carolina State U.
  E. N. Pinson, Bell Telephone Labs.
  S. Rosen, Purdue U.
  D. M. Young, Jr., U. Texas at Austin
Reactor Analysis and Safety Division Review Committee:
  S. Baron, Burns and Roe, Inc.
  W. Kerr, U. Michigan
  M. Levenson, Electric Power Research Inst.
  S. Levy, S. Levy, Inc.
  R. B. Nicholson, Exxon Nuclear Co., Inc.
  D. Okrent, U. California, Los Angeles
  N. C. Rasmussen, Massachusetts Inst. Technology